

NUCLEAR MAGNETIC RELAXATION
STUDIES OF LECITHIN BILAYERS

Thesis by
Gerald W. Feigenson

In Partial Fulfillment of the Requirements
for the Degree of
Doctor of Philosophy

California Institute of Technology
Pasadena, California

1974

(submitted November 26, 1973)

To Vivian

ACKNOWLEDGMENT

I would like to thank Karen Gleason for typing this thesis on short notice.

I would like to acknowledge the technical help of Bob Vaughan.

Professor Sunney I. Chan provided assistance during the course of this work, and the National Institutes of Health provided financial support.

I would like to thank Max Delbrück and Annette Smith for many stimulating discussions, and for their active encouragement.

My friendship with Charlie Seiter and our collaboration during this work have been most enjoyable for me.

I am grateful to my wife Vivian. She has worked hard for a long time.

ABSTRACT

In an effort to elucidate the state of molecular motion in aqueous lecithin systems, the nuclear magnetic relaxation properties of unsonicated lecithin crystal and liquid crystal phases have been investigated. The presence of a narrow component in the nmr spectrum of aqueous lamellar lecithin crystals is taken to indicate a significant degree of motion of the lecithin methyl groups in this solid phase. Also in the crystal state of lecithin, nmr linewidth measurements, together with thermal analysis experiments appear to indicate that a structural rearrangement of either the lecithin or the bound water takes place, which is not accompanied by an increase in molecular mobility. Delayed Fourier Transform and wide-line nmr experiments show that at the crystal \rightarrow liquid crystal (bilayer) phase transition temperature, the lecithin choline methyl, terminal methyl, and hydrocarbon chain methylene protons are all simultaneously mobilized. A previously noted field dependence of the proton magnetic resonance linewidth of aqueous lecithin bilayers is shown to be accounted for by the chemical shift differences among the various kinds of protons. Spin lattice relaxation rates have been measured for these protons as a function of temperature and frequency, and these data have been interpreted in terms of models for the segmental motion of the choline head groups and the hydrocarbon chains. The influence of spin diffusion on the relaxation behavior of the various protons is also discussed.

TABLE OF CONTENTS

<u>Part</u>	<u>Title</u>	<u>Page</u>
I	Introduction	1
II	Physical Methods	14
	1. Electron spin resonance	15
	2. X-ray diffraction	16
	3. Fluorescence	19
	4. Thermal analysis	20
	5. NMR linewidth studies	20
	6. NMR spin-lattice relaxation studies	24
III	Experimental	28
	1. Materials	28
	2. Instrumentation	29
IV	Results	30
	1. Below the phase transition temperature	30
	2. Above the phase transition temperature	41
	3. Delayed Fourier Transform spectra	46
	4. T_2	60
	5. T_1	60
V	Discussion	66
	1. Field-dependent lineshape	66
	2. Molecular mobility at the Kraft temperature	71
	3. Molecular motion in the crystal phase of lecithin	72
	4. Methyl groups above the Kraft temperature	77
	5. Comparison of pmr and D. T. A. results	79
	6. The question of spin diffusion	80
	7. Interpretation of T_1 data	87
	8. Segmental motion of the hydrocarbon chain	93
VI	Conclusion	95
	References	98
	Propositions	104

I. Introduction

Biological membranes have two distinct functions: they act as barriers to molecular diffusion, and they provide a surface for chemical reactions. As barriers to diffusion, biomembranes separate the cell from its surroundings and separate the parts of a cell from each other. The selective permeability of the cell membrane supplies the cell with nutrients, allows the cell to rid itself of waste materials, and enables the cell to respond to the environment by variation of membrane permeability. As a reaction surface, the membrane reduces the randomness of a chemical reaction, and thereby increases the reaction rate. The specialized biological membranes combine the functions of selective permeability and increased chemical reaction efficiency. For example, the photosynthetic apparatus of chloroplasts and the oxidative phosphorylation mechanism in mitochondria both involve the physical separation of various solutes together with chemical reactions on or within the membrane. ⁽¹⁾ Likewise, nerve and muscle membranes couple a surface chemical reaction to the alteration of the membrane permeability characteristics.

The biomembrane is made up of proteins, lipids and carbohydrates. The relative amounts of these constituents are different for the different kinds of membranes. ⁽²⁾ These chemical constituents have been studied separately from each other and in various artificial combinations. The proteins present formidable difficulties

to their characterization because they are, for the most part, lipophilic, thus preventing the use of conventional protein techniques which use water as the solvent. ⁽³⁾ The use of surface active substances such as sodium dodecyl sulfate and sodium cholate has proven useful for separating proteins, especially enzymes, from natural membranes. ⁽⁴⁾ The membrane carbohydrates are also difficult to study because of the difficulty of purification, the lack of criteria for purity, and the problem of removing non-carbohydrate impurities. ⁽⁵⁾

The lipid components of biomembranes have been better characterized. These are usually either neutral lipids, largely cholesterol, and phospholipids. ⁽²⁾ Some of the more common membrane lipids are shown in Figure 1. The amphiphilic nature of the phospholipids gives these molecules surface active properties common to other amphiphiles such as detergency and micelle-forming ability. In addition, amphiphilic molecules form various phases with water. ⁽⁶⁾

One of the phases which amphiphiles form with water is the bilayer phase, also called the neat phase or the mesomorphic lamellar phase. The description of the bilayer phase as intermediate between crystalline and amorphous was made by de Broglie and Friedel in 1923. ⁽⁷⁾ These investigators established for aqueous potassium and ammonium oleate, using low-angle x-ray diffraction measurements, that these molecules formed a phase containing bilayer planes of molecules, with a fixed distance between the planes.

FIGURE 1

The structures of some common membrane lipids. Hydrogen atoms attached to carbon atoms are not shown, for the sake of clarity.

- (A) Phosphatidyl ethanolamine
- (B) Phosphatidyl serine
- (C) Phosphatidyl inositol
- (D) Phosphatidyl choline (lecithin)
- (E) Cardiolipin
- (F) Sphingomyelin
- (G) Cerebroside
- (H) Cholesterol

The hydrocarbon chains of molecules in the bilayer phase were thought to be parallel to each other and perpendicular, or inclined at a slight angle, to the plane of the head groups, as shown in Figure 2. Using optical methods, McBain established that soaps in general can form the bilayer phase, or various other phases depending on the temperature and the water content. (8, 9)

The bilayer phase is interesting to others besides soap chemists because biological lipids can form a bilayer phase with water. (10) An important question, then, is whether lipids do exist in the bilayer phase in biological membranes.

Gorter and Grendel proposed in 1924 that cells ". . . are covered by a layer of fatty substances that is two molecules thick." (11) This proposition was based on a comparison of the area which the lipids extracted from red blood cells could cover with a monomolecular layer, with the estimated red blood cell surface area. It was found that sufficient lipid was present to cover the cell exactly twice.

Davson and Danielli elaborated the Gorter and Grendel model by assigning the membrane proteins to sheets covering both sides of the lipid bilayer, as shown in Figure 3. (12) This model explained the low cellular interfacial tension measurements, and incorporated all of the known membrane components into a simple physical description of membrane structure.

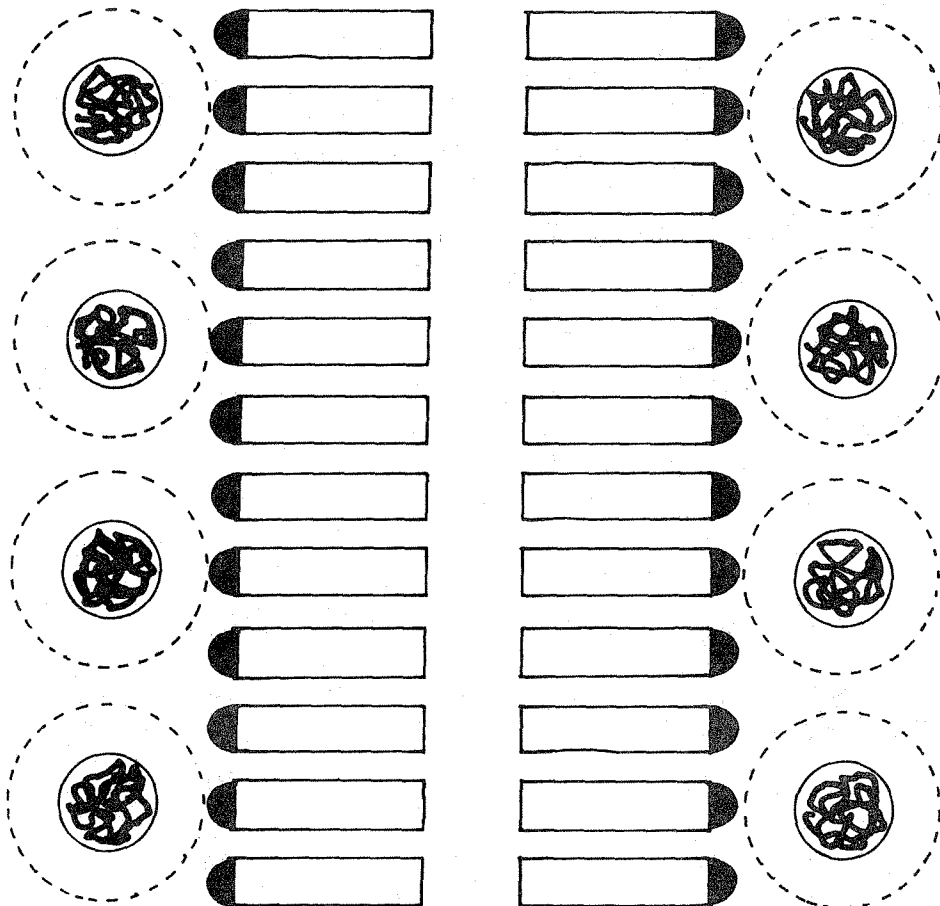
Apparent confirmation of the biological reality of the Davson-Danielli model came from x-ray diffraction measurements on myelin. (13) Later, electron microscopic evidence of a trilaminar

FIGURE 2

Schematic illustration of the formation
and structure of the bilayer phase of
lecithin.

FIGURE 3

**The Davson-Danielli model of a
biological membrane.**



PROTEIN

LIPID

PROTEIN

pattern around cells and cell organelles in many different biological systems was the currency of speculation that the Davson-Danielli membrane model, with a different class of proteins on either side of the membrane, was applicable to perhaps all biological membranes. (14)

Criticism of the universality of the Davson-Danielli model has been offered by several investigators, but perhaps most cogently by Korn. (2, 15) The principal arguments advanced by Korn are (1) the supposed correspondence between the area of a cellular lipid bilayer and the cell surface area is in error by 30%, and (2) the electron photomicrographs are misleading, because sample preparation and staining cause artifacts.

Korn and others have argued for less simple, less general membrane models which picture extensive lipid-protein interactions, perhaps to the complete exclusion of the lipid bilayer. Association of membrane lipids and proteins in discrete, water soluble units has been demonstrated in vitro. (16) Evidence that lipids may be found in several different physical locations in membranes has been obtained from phospholipase C treatment of red blood cell membranes. (17) Sheetz, using high resolution proton magnetic resonance techniques, has shown that lipids are present at the surface of the red blood cell, in direct contrast to the interior location of lipids in the Davson-Danielli model. (18)

Despite the evidence above that a bilayer phase encased in protein is not the only location of lipids in membranes, there is now

direct confirmation of the presence of bilayers in biological membranes. Steim et al. used differential scanning calorimetry to observe a phase change in *Mycoplasma laidlawii* membranes which corresponded in temperature and in enthalpy change to the crystal → bilayer (liquid crystal) phase transition for the extracted membrane lipids in water. ⁽¹⁹⁾ Recently, Blazykt and Steim showed that differential scanning calorimetry could detect the crystal → bilayer transition in a variety of mammalian membranes. ⁽²⁰⁾ X-ray diffraction ⁽²¹⁻²³⁾ and spin label studies ^(24, 25) have also confirmed the biological reality of the bilayer phase in membranes.

The current interest in understanding the details of structure and function of biological membranes has prompted studies of model membrane systems, and the lamellar liquid crystalline phase of lecithin and water increasingly is being used as a model for biological membranes. ⁽²⁶⁻³⁰⁾ Coarse aqueous liquid crystal dispersions can be irradiated ultrasonically to produce bilayer vesicles which are useful models for studying membrane function, especially transport. ^(26, 31) However, there is strong evidence that, at the molecular level, the vesicle bilayer is significantly disordered because of the high curvature of these small particles. ^(32, 33) For this reason, coarse aqueous dispersions of lamellar liquid crystals, sometimes referred to as "multilayers", are better models of membrane structure, though they are not suitable for transport studies because of the absence of a well-defined inside and outside.

Nuclear magnetic resonance (nmr) is a method of established

usefulness for studying molecular interactions. Furthermore, nmr is sensitive to the details of molecular motion. For these reasons, there is much interest in using nmr to investigate membrane systems. Lipid model membranes, (34-40) as well as erythrocyte⁽¹⁸⁾ and mitochondrial membranes, (28) have been studied with nmr.

Many previous nmr studies of model membranes have been done on ultrasonicated lipid bilayer vesicles, because such systems give rise to sharp nmr lines. (33, 41) However, the nmr spectra of real biomembranes are dominated by broad resonances. (18, 28) These spectral differences have been shown to be indicative of structural differences. (32) In this respect, the nmr spectra of biomembranes contain features which are just those found in the nmr spectra of unsonicated lecithin multilayers.

However, experimental and theoretical difficulties exist which preclude the straightforward application of nmr techniques to obtain information about these complex systems. The aqueous lecithin bilayer phase, although it is a simple model system from the biologist's point of view, is a most complex spin system from the standpoint of the nmr spectroscopist. There are ¹³C, ³¹P, and ¹H spin systems. Considering just the proton spin system, there are spins with different chemical shifts, there are spins in various motional states, and there are two-spin (methylene) and three-spin (methyl) systems which possess distinctly different kinds of nmr spectra. Finally, the intermediate state of molecular motion which is characteristic of the liquid crystalline phase has not yet

been correlated with nmr parameters in the thorough and detailed manner of the very slow motion in a solid or the fast motion in a liquid.

As mentioned above, one aspect of the complexity of the lecithin bilayer system is the presence of chemically shifted protons. In the bilayer phase, the distinguishable protons are those of the choline methyl polar head group, the methylene protons, and the methyl group protons of the hydrocarbon side chains. The existence of these chemical shifts permits, in principle, the determination of the motional state of the various parts of the lecithin molecule. Unfortunately, because these different proton resonances overlap severely, the experimentally determined nmr parameters for each spin species such as linewidth and spin-lattice relaxation time (T_1) may contain significant unsuspected contributions from the other spins.

Another way in which the measured nmr parameters become less simply related to the properties of a particular spin species is through the influence of one spin on the relaxation of its neighboring spins. The most important manifestation of this coupling of spins is that intrinsic differences in T_1 are either reduced or eliminated, thereby making more difficult the interpretation of the measured value of T_1 .

A significant instrumental problem is that the proton magnetic resonance (pmr) spectra of aqueous lecithin bilayers contain both solid-like and liquid-like features, i. e., very broad resonances

together with much sharper resonances.⁽³⁴⁾ This spectral complexity is a result of the effect of restricted motion on the choline and terminal methyl three-spin systems. The pmr spectrum of such a spin system may consist of a narrow central resonance superimposed on a broad background resonance.⁽⁴²⁾ This means that nmr spectrometers capable of observing the large frequency range characteristic of solids must be used, as well as the more conventional high resolution nmr spectrometers, which can resolve small frequency differences between resonances and small changes in linewidths and signal intensities.

It is the purpose of this work to explore the application of nmr techniques to determine the structural and the motional properties of the aqueous lecithin bilayer phase. The emphasis will be on the usefulness of certain nmr techniques and the limitations of others as applied to this complex system.

II. Physical Methods

The aqueous lecithin bilayer system has been studied with a variety of techniques, including nmr. Some of the pertinent findings of these methods are briefly reviewed in this section. In general, it may be said that these techniques indicate that there is considerable molecular mobility in the bilayer phase as compared with the crystalline phase of lecithin, although the extent of this mobility cannot be described in detail.

1. Electron spin resonance. Stable free radicals have been used as electron spin resonance (esr) probes of molecular motion. The esr spectrum of the small, hydrophobic molecule TEMPO (2, 2, 6, 6-tetramethyl piperidine-1-oxyl) seems to indicate the presence of fluid hydrophobic regions in lecithin multilayers. ⁽⁴³⁾ The TEMPO molecule tumbles isotropically in multilayers with a correlation time of 10^{-9} - 10^{-11} sec. The partition of TEMPO into the bilayer is increased in the presence of some anaesthetics and decreased by cholesterol and by gramicidin S. ⁽⁴³⁾ This result was interpreted to mean that anaesthetics disordered the bilayer structure, whereas cholesterol and gramicidin S further ordered the bilayer. TEMPO has also been used to monitor the crystal \rightarrow bilayer phase transition, since this free radical is much less soluble in the crystal phase of lecithin. ⁽⁴⁴⁾

Nitroxide esr labels have been attached to fatty acid and to lecithin hydrocarbon chains in order to investigate molecular conformation and motion in the bilayer phase. ^(45, 46) The most general statement of the findings of this technique is that there is little molecular motion below the crystal \rightarrow liquid crystal phase transition temperature (also called the Kraft temperature) and considerable motion above this temperature. Hubbell and McConnell have developed a model in which there is rapid motion around the hydrocarbon chain axis together with trans-gauche interconversion giving rise to off-axis motion. ⁽⁴⁵⁾ It is proposed in this model that the probability of a trans-gauche interconversion is higher with

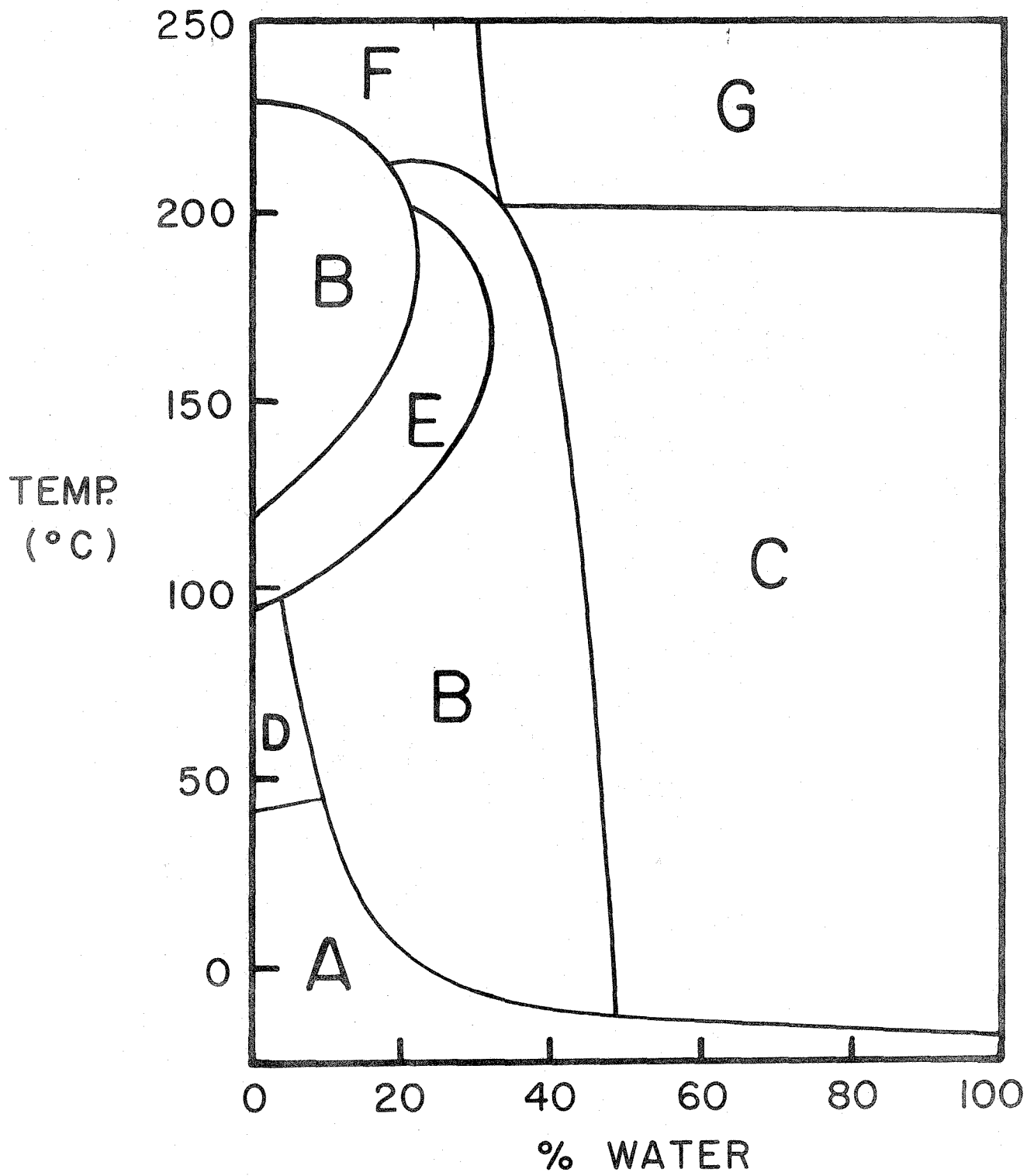
increasing distance from the polar head group, thus giving rise to greatest molecular disorder in the center of the hydrocarbon region of the bilayer.

2. X-ray diffraction. The x-ray diffraction pattern from lecithin below the Kraft temperature shows a sharp 4.2 Å band characteristic of fully extended hydrocarbon chains.⁽⁴⁷⁾ Above the Kraft temperature, there is instead a diffuse 4.6 Å band, which is also found for liquid hydrocarbons.⁽⁴⁷⁾ However, the mobility of the lecithin molecules is not revealed by x-ray diffraction measurements, because the time scale of this technique is usually several hours.

To better understand the phase behavior of lecithin, the binary phase diagram of egg yolk lecithin and water is given in Figure 4. This phase diagram was constructed from x-ray diffraction data from Luzzati,⁽⁴⁸⁾ Reiss-Husson,⁽⁴⁹⁾ and Small.⁽⁵⁰⁾ In region A a single lamellar crystalline phase exists, with the lecithin hydrocarbon chains rigid and oriented approximately perpendicular to the plane of the lamellae. Region B contains a single phase, the bilayer phase. In region C there are two phases in equilibrium, pure water and a bilayer phase of the composition given by the intersection of a tie line with the boundary of region B. Region D is a complex part of the phase diagram, consisting of seven different one or two phase regions. Region E is a single phase, the cubic isotropic phase, in which spherical aggregates of lecithin surround

FIGURE 4

Binary temperature-composition phase diagram of egg yolk lecithin and water. The various regions of the diagram are described in the text.



small amounts of water. In region F the lecithin and water form a single phase of liquid showing no long-range order. Region G contains two liquid phases, pure water together with a lecithin and water phase.

X-ray diffraction measurements have indicated that lipids in the bilayer phase are present in membranes from *M. laidlawii*,⁽²¹⁾ *E. coli*,⁽²³⁾ mammalian cells,⁽²⁰⁾ erythrocytes,⁽⁵¹⁾ and frog retinal rod outer segments.⁽⁵²⁾ In the latter, rhodopsin shows up distinctly from the lipids and does not appear to be localized on one side of the membrane. The erythrocyte x-ray diffraction pattern is quite similar to that for phospholipids together with cholesterol, which is in accord with the high cholesterol content of these membranes.⁽⁵¹⁾

3. Fluorescence. Fluorescent probes, such as ANS (8-anilino-1-naphthalene sulfonate), which are sensitive to the polarity and mobility of their molecular environment, have been used to study the lecithin crystal \rightarrow liquid crystal phase transition. Studies by Sackmann and Träuble have indicated that the lecithin polar head groups are more mobile and are farther apart in the bilayer phase than in the crystal phase.⁽⁵³⁾ The partition of ANS into the bilayer is enhanced by cations and by some anaesthetics.⁽⁵⁴⁾ In real biological membranes, e. g. erythrocytes,⁽⁵⁵⁾ the fluorescence behavior of ANS is similar to that in bilayers. However, there is some uncertainty about the location of ANS in real biomembranes, though it is believed to be in the hydrophobic regions of the lipids and the

proteins. (54, 56)

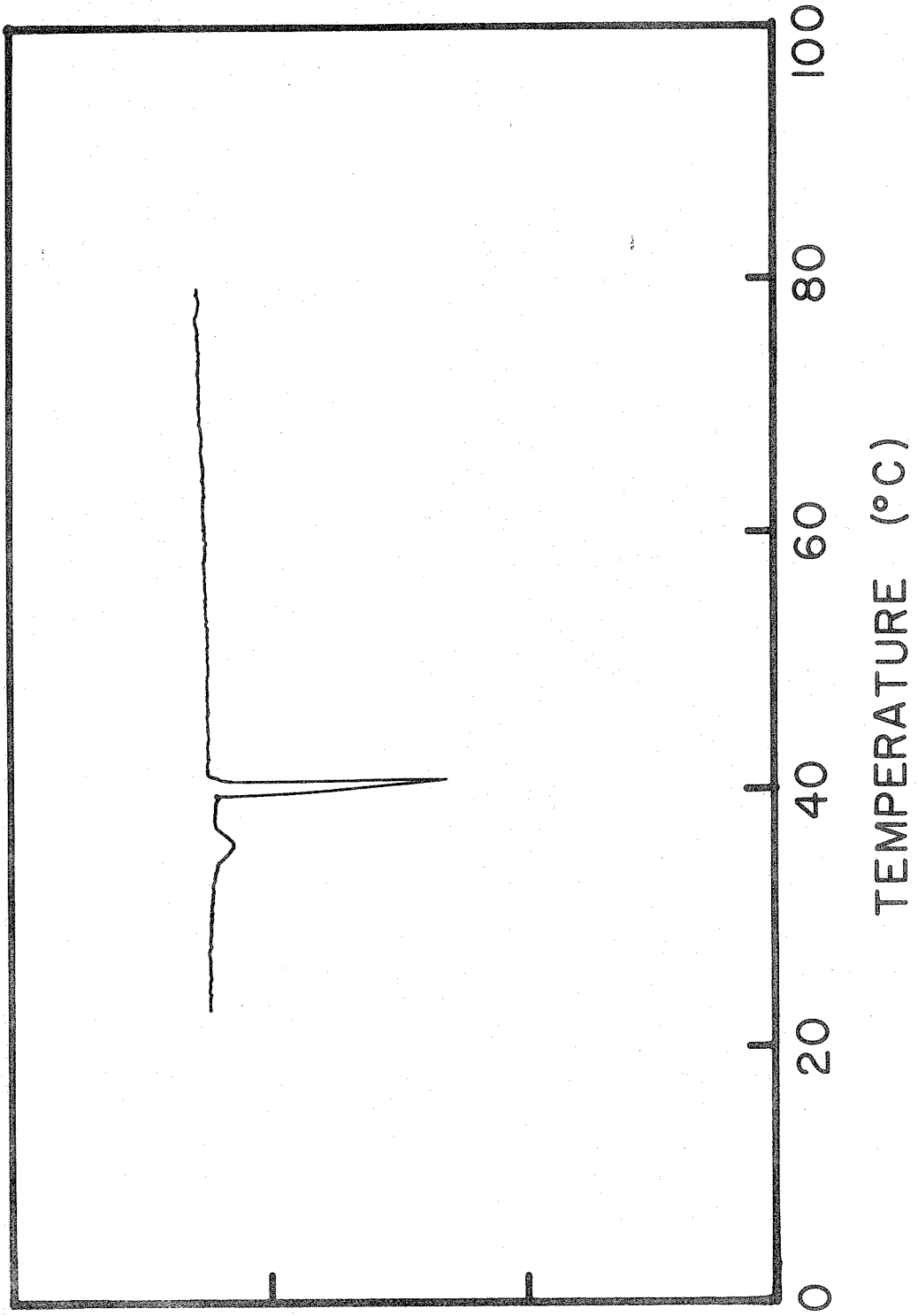
4. Thermal analysis. Differential scanning calorimetry (D. S. C.) and differential thermal analysis (D. T. A.) have been used to monitor the crystal \rightarrow liquid crystal lecithin phase transition. (57, 58) A D. T. A. plot for aqueous dipalmitoyl lecithin is shown in Figure 5. The large, sharp peak at 41.5°C has been interpreted as arising from the heat absorbed during the melting of the hydrocarbon side chains. (57) For lecithins with different hydrocarbon chain lengths, D. S. C. results appear to show that the enthalpy and the entropy of the phase transition correlate with chain length. However, the increase in heat capacity of lecithins from the crystal to the liquid crystal state is about 5 cal deg⁻¹ (mole of hydrocarbon chain)⁻¹, whereas the heat capacity increase upon melting of a normal alkane is \sim 17 cal deg⁻¹ mole⁻¹. This result has been interpreted by Hinz and Sturtevant to indicate a restricted state of motion in the bilayer phase, compared with the state of motion of a liquid hydrocarbon. (58)

The small pre-phase transition peak seen in Figure 5 between 35° and 38°C has been observed by several other investigators. It has been ascribed to the onset of polar head group motion in the lecithin molecule⁽⁵⁷⁾ or to the onset of mobility in the water bound at the bilayer surface. (59)

5. NMR linewidth studies. Nuclear magnetic resonance (nmr) linewidth and spin-spin relaxation time measurements are sensitive to the details of molecular motion. When molecular

FIGURE 5

Differential thermal analysis plot
of aqueous dipalmitoyl lecithin
(heating).



DIFFERENTIAL
TEMPERATURE

TEMPERATURE (°C)

motion is rapid ($< 10^{-9}$ sec), the nmr linewidths are narrow, unless overlapping chemical shifts are present. Restricted or slow molecular motion leads to incomplete averaging of dipole-dipole interactions and of chemical shift anisotropies. Other line-broadening mechanisms, such as magnetic field inhomogeneities and molecular diffusion through magnetic field gradients are sometimes important. In order to use the lineshape to determine the state of molecular motion, it is first necessary to establish which line-broadening mechanisms are important for the system under investigation.

PMR linewidth measurements have been used to study molecular motion in the bilayer phase. The broadness of the pmr resonance for several different soap molecules in the bilayer phase was investigated by Lawson and Flautt.⁽³⁸⁾ The width of the resonance was attributed to magnetic dipole-dipole interactions between protons, incompletely averaged by slow molecular motion. The unusual shape of the line was thought to be caused by contributions to the signal from protons along the hydrocarbon chain with a distribution of correlation times.

The broad resonances from the pmr spectra of lecithin bilayers were also at first attributed to dipole-dipole interactions.⁽³⁹⁾ However, the discovery that the pmr linewidth of lecithin bilayers was apparently magnetic field strength dependent,^(40, 41, 60, 61) together with the dependence of T_2 on pulse spacing, as determined by the Carr-Purcell method,⁽⁶¹⁾ brought forth alternative explanations for the spectral line-broadening. Various investigators

avored magnetic field inhomogeneities in the sample, ⁽⁶⁰⁾ molecular diffusion through local magnetic field gradients, ⁽⁶¹⁾ and chemical shift anisotropy ⁽⁴¹⁾ as the dominant line-broadening mechanism. These explanations gave rise to the contention that the bilayer was actually fluid like a hydrocarbon liquid, ⁽⁴¹⁾ and that the source of broad pmr signals was not slow or restricted molecular motion, but rather the unusual properties of the bilayer sample, e. g. anomalous magnetic field gradients at the phase boundaries. ^(40, 60)

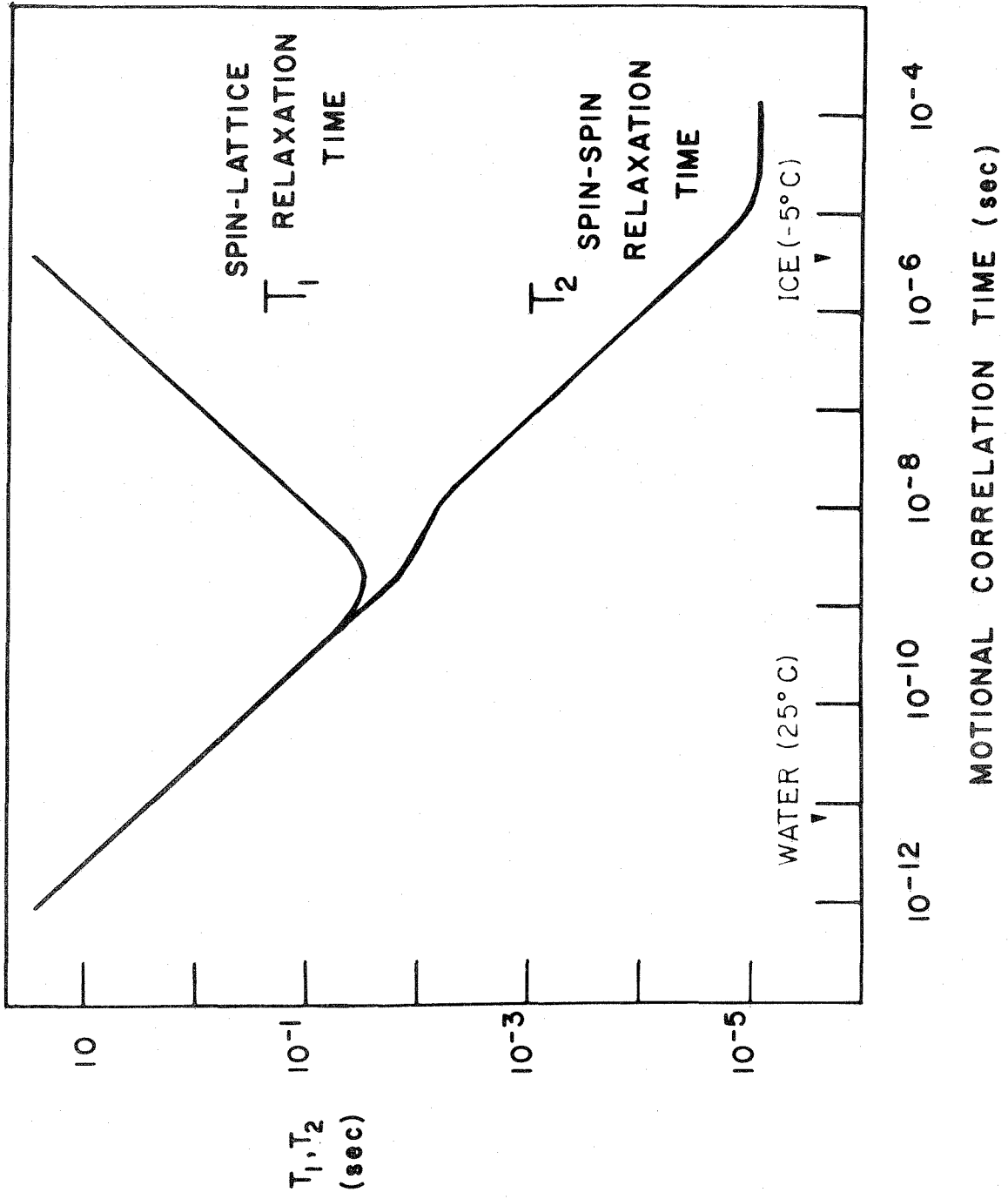
Sonicated lecithin bilayer vesicles have been used as biomembrane models by numerous investigators, using various physical methods. ^(26, 31, 33, 62) Recent nmr studies have shown that the structure of these vesicles is significantly more disordered than is the structure of unsonicated lecithin bilayers or of most biomembranes. ^(32, 33) The present investigation has been confined to the study of unsonicated bilayers, and all references to bilayers refer to unsonicated bilayers.

6. NMR spin-lattice relaxation studies. The spin-lattice relaxation time (T_1) is sensitive to the frequency of molecular motion, as shown in Figure 6, and also to the external magnetic field strength. Because T_1 is not affected by local static magnetic fields, but rather by time dependent magnetic fields, it is far less sensitive than is T_2 to restrictions on molecular motion which have a time-independent component of the dipole-dipole interaction.

For the crystal phase of soaps, van Putte showed that

FIGURE 6

The variation of the nuclear magnetic relaxation times, T_1 and T_2 , as a function of the motional correlation time.



deuteration of the terminal methyl group caused a large increase in T_1 , thus indicating that these methyl groups were mobile even in the crystal phase, whereas the rest of the molecule was relatively immobile. ⁽⁶³⁾ Daycock et al. claimed that T_1 measurements showed that only the choline methyl groups were mobile in the crystal phase of lecithin, and that these protons relaxed the entire lecithin proton system. ⁽⁶⁴⁾ However, in these latter experiments the instruments used were not appropriate for solids: the free induction decay had dropped to about 10% of its initial value by the time data collection had begun.

Measurements of T_1 for aqueous egg lecithin bilayers by Penkett et al. showed the very interesting property of continuous variation, with no abrupt change, as the crystal \rightarrow bilayer phase transition was traversed. ⁽⁴¹⁾ Over this same temperature range, T_2 was discontinuous, becoming approximately a factor of ten longer in the bilayer phase. ⁽⁴¹⁾ These investigators used these results to argue that motional modulation of dipolar interactions was not the source of spectral line-broadening. However, here again the experimental design was not appropriate for solids (or even semi-solids), although it would have been suitable for liquids. That is, the saturation-recovery equipment was of too low power to saturate the entire signal, and the high-resolution spectrometer had too narrow a sweep width to detect the entire signal.

In addition to the above experimental difficulties, the unusual state of motion of lecithin in the bilayer phase presents difficulties

in the interpretation of T_1 measurements. The different parts of the molecule may be in quite different motional states, and thus could have different T_1 values. The motion of any given part of the molecule is almost certainly anisotropic, and thus should be characterized by two correlation times. For example, the methyl rotor may be reorienting rapidly about its rotor axis and undergoing off-axis motions at a much slower rate. As shown in detail in a later section, such anisotropic motion can lead to complex T_1 behavior.

III. Experimental

1. Materials. Dimyristoyl lecithin from Nutritional Biochemicals, Inc., and dipalmitoyl lecithin, obtained from Calbiochem, gave a single spot by thin-layer chromatography, and were used without further purification. Egg yolk lecithin was prepared by the method of Singleton et al. ⁽⁶⁵⁾ Deuterium oxide, 100.0% ^2H , from Dia-Prep, was used in the preparation of dipalmitoyl and egg lecithin multilayers. Deuterium oxide, 99.7% ^2H from Columbia Organics, was used for samples of dimyristoyl lecithin. Valinomycin, A grade, and DL-glutamic acid hydrate, A grade, from Calbiochem were also used without further purification. CaSO_4 , reagent grade, was obtained from Matheson, Coleman and Bell.

The pmr samples were prepared by extensive agitation of lecithin and D_2O in an nmr tube, using a vortex mixer. Some of

these samples also contained a capillary of TMS (tetramethylsilane) for a chemical shift standard and a capillary of ethylene glycol for a temperature standard. A capillary of CHCl_3 doped with 2, 2-diphenyl-1-picrylhydrazyl (DPPH) was used as an intensity standard when required.

2. Instrumentation. CW spectra recorded at 220 MHz were obtained on a Varian HR-220 spectrometer equipped with a variable temperature accessory, operating in the frequency sweep mode.

Spectra recorded at 100 MHz in the continuous wave (cw) mode were obtained on a Varian HA-100 spectrometer, modified to sweep the magnetic field over a range of up to 25 gauss ($\sim 100,000$ Hz). In this modification, the audio modulation to the probe was disconnected, thereby eliminating the 2 kHz sidebands. The Varian slow sweep unit was used to sweep the magnetic field. The phase-detected signal from the receiver was amplified by a Hewlett Packard model 463A Precision Amplifier, and went then to the recorder. This arrangement of the spectrometer was thus not field-frequency locked, and so was sensitive to drift of the magnetic field. Also, the absence of audio modulation and detection allowed a considerable amount of noise, as well as large DC (baseline) fluctuations in the recorded spectrum. The sample was not spun, because of the unfiltered low frequency noise thereby introduced.

The delayed Fourier Transform spectra were obtained on Varian HA-100 and HR-220 spectrometers, equipped with Fourier

Transform accessories and interfaced to a Varian 620i computer. A data collection delay time of 475 μsec was used in the Delayed Fourier Transform measurements. (66)

Pulse nmr measurements were made on a system consisting of a model BA Pulse Programmer, model BK Superhet Interface, and model BR 250 watt transmitter, all from Tomlinson Research Instruments Corp. Probes for this system, of homemade construction, will be described briefly. The single-coil probe circuit shown in Figure 7 was used for all of the probes. The probe body was machined from a single piece of aluminum, with an aluminum plate cover attached with screws. Depending upon the sample size and the frequency of operation, the inductor consisted of between four and twenty-three turns of 22 gauge copper wire. The two capacitors shown in the probe circuit of Figure 7 were chosen so that the circuit was resonant at the desired operating frequency and also presented an impedance of approximately 200 Ω , as determined using a Hewlett Packard Vector Impedance Meter model 4815A. Data were recorded by photographing the oscilloscope trace of the phase-detected free induction decay.

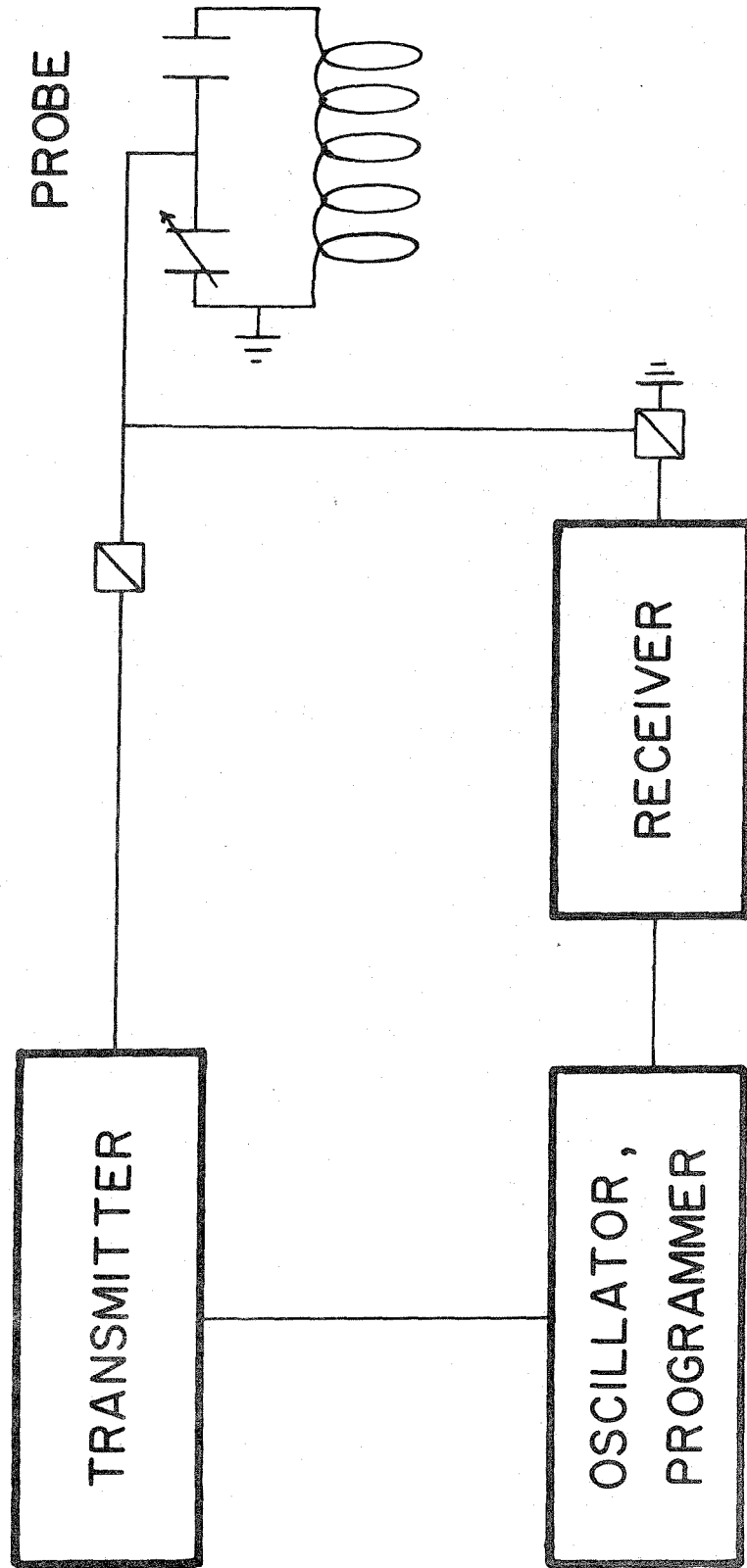
Differential thermal analysis measurements were obtained on a DuPont model 900 Differential Thermal Analyzer.

IV. Results

1. Below the phase transition temperature. In order to

FIGURE 7

Schematic diagram of the pulse
nmr equipment used in the relaxa-
tion time experiments.



examine the molecular motion of lecithin in its crystal state, the modified HA-100 spectrometer was used to obtain a 100 MHz cw spectrum of aqueous dipalmitoyl lecithin below the Kraft temperature, shown in Figure 8a. The sweep width was calibrated from the measured frequency difference between TMS and CHCl_3 doped with DPPH. This spectrum contains two broad resonances, one of which is $21,000 \pm 1000$ Hz in width and comprises approximately 75% of the total signal intensity, while the other resonance is 2400 ± 300 Hz in width and comprises approximately 25% of the lecithin signal. The sharp resonances in Figure 8a, starting with the one farthest downfield and then progressing upfield, are from protons in CHCl_3 doped with DPPH, the hydroxyl protons of ethylene glycol, the methylene protons of ethylene glycol, and finally the protons of TMS.

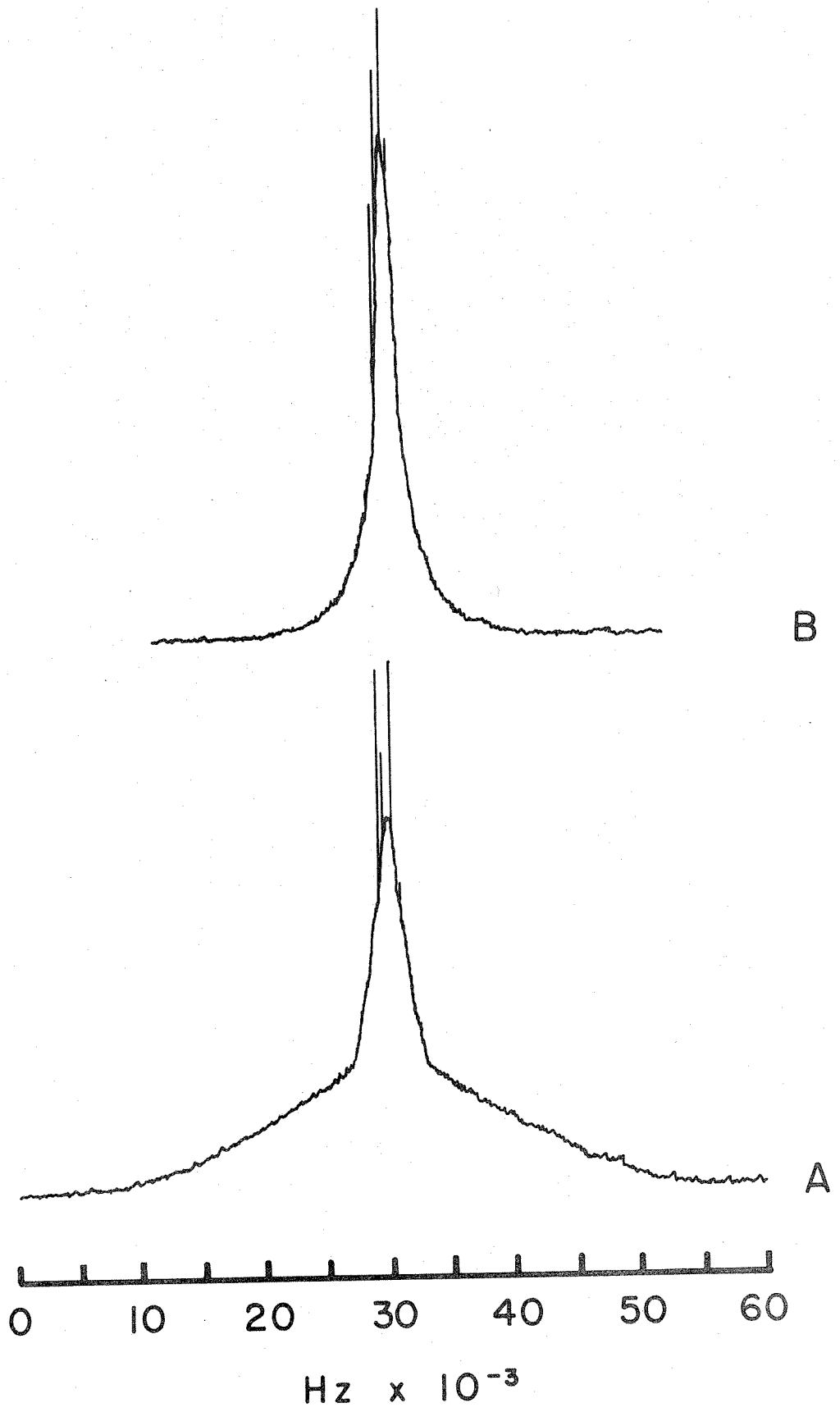
In Figure 8b the spectrum of the same sample is shown above the Kraft temperature. As in Figure 8a, there appear to be two broad components, although these are sharper and less distinct from each other than are the broad resonances in Figure 8a. As shown in detail later in this work, it is not possible to determine the linewidth and signal intensities from this cw spectrum.

In order to more closely examine the lineshape behavior below the Kraft temperature, especially in the region of the pre-phase transition peak observed with differential thermal analysis, the pmr spectra of an aqueous dipalmitoyl lecithin sample were recorded at 220 MHz using a 20,000 Hz sweep width. The HR-220 spectrometer

FIGURE 8

100 MHz proton magnetic resonance
spectra of aqueous dipalmitoyl lecithin
(a) spectrum recorded at 24°C, and
(b) spectrum recorded at 55°C.

35



allowed more convenient temperature variation, and a calibrated and more stable sweep range than did the modified HA-100. A series of spectra taken at different temperatures is shown in Figure 9. The broadest resonance corresponds to the 2400 Hz wide peak in Figure 8a. However, the 21,000 Hz wide peak of Figure 8a is not seen in Figure 9 because the maximum sweep range of 20,000 Hz is too narrow to make such a broad peak discernible. Instead, this broad peak appears as a slight curvature in the spectral baseline. The broad peak which is visible in Figure 9 decreases with no abrupt changes in linewidth from 2500 ± 200 Hz at 33°C to 1800 ± 200 Hz at 41°C .

To investigate the behavior of water bound in the lecithin bilayer, again with the intention of examining the temperature region in which D. T. A. shows the pre-phase transition peak, pmr spectra at 220 MHz were recorded for a sample of dipalmitoyl lecithin containing 25% by weight H_2O . These pmr spectra are shown as a function of temperature in Figure 10. The large resonance in these spectra is from the H_2O . The linewidth of this peak remains constant at 490 ± 10 Hz over the temperature range $30^\circ\text{-}39^\circ\text{C}$. Above the Kraft temperature of 41.5°C the water linewidth is difficult to measure precisely because of the presence of lecithin resonances, but it does not change greatly from its value below 41.5°C .

Because the nmr studies showed no lineshape changes in the range of temperature corresponding to the D. T. A. pre-phase transition peak, thermal analysis experiments were performed in

FIGURE 9

220 MHz cw spectra of aqueous
dipalmitoyl lecithin below the phase
transition temperature.

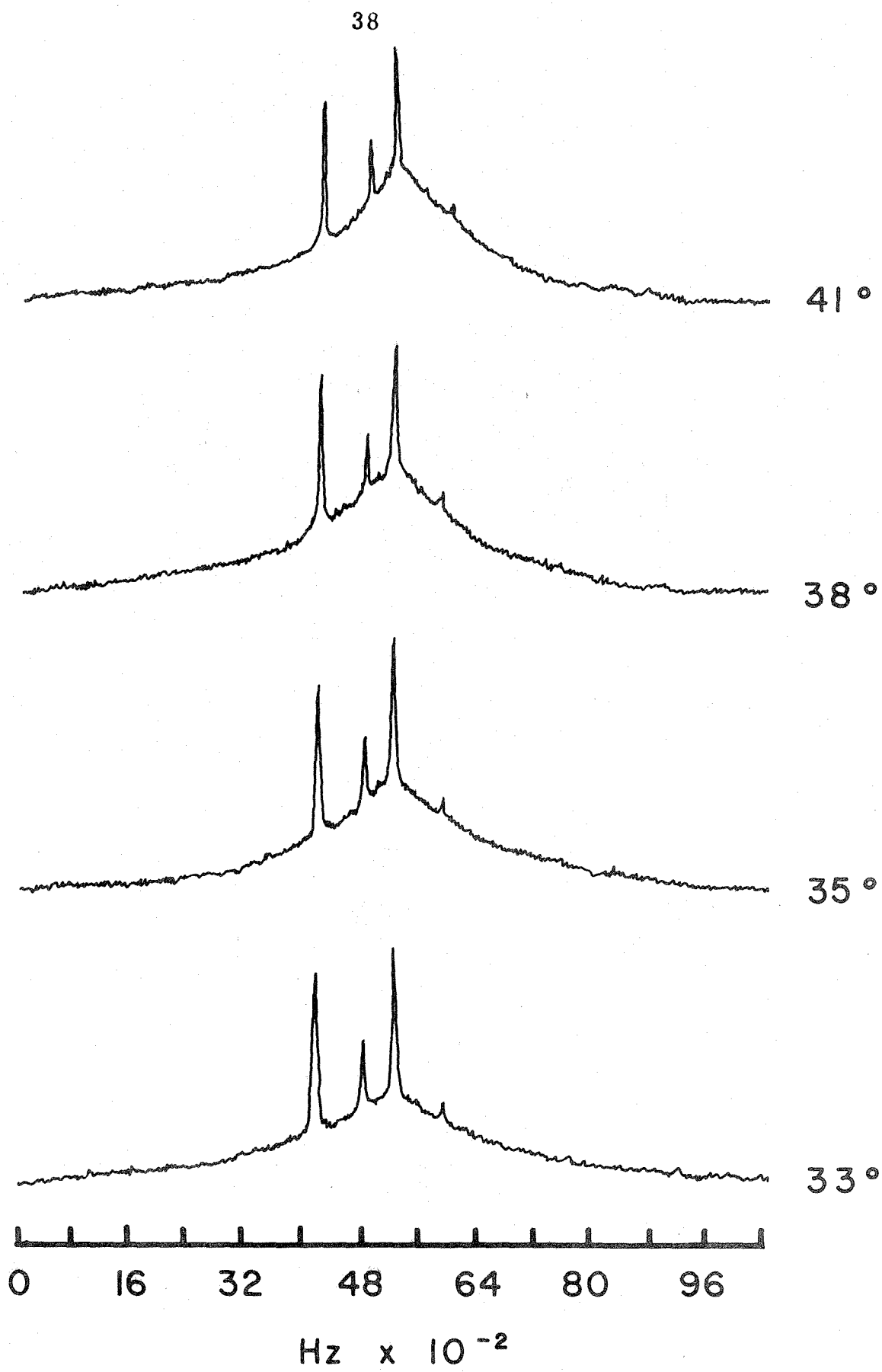
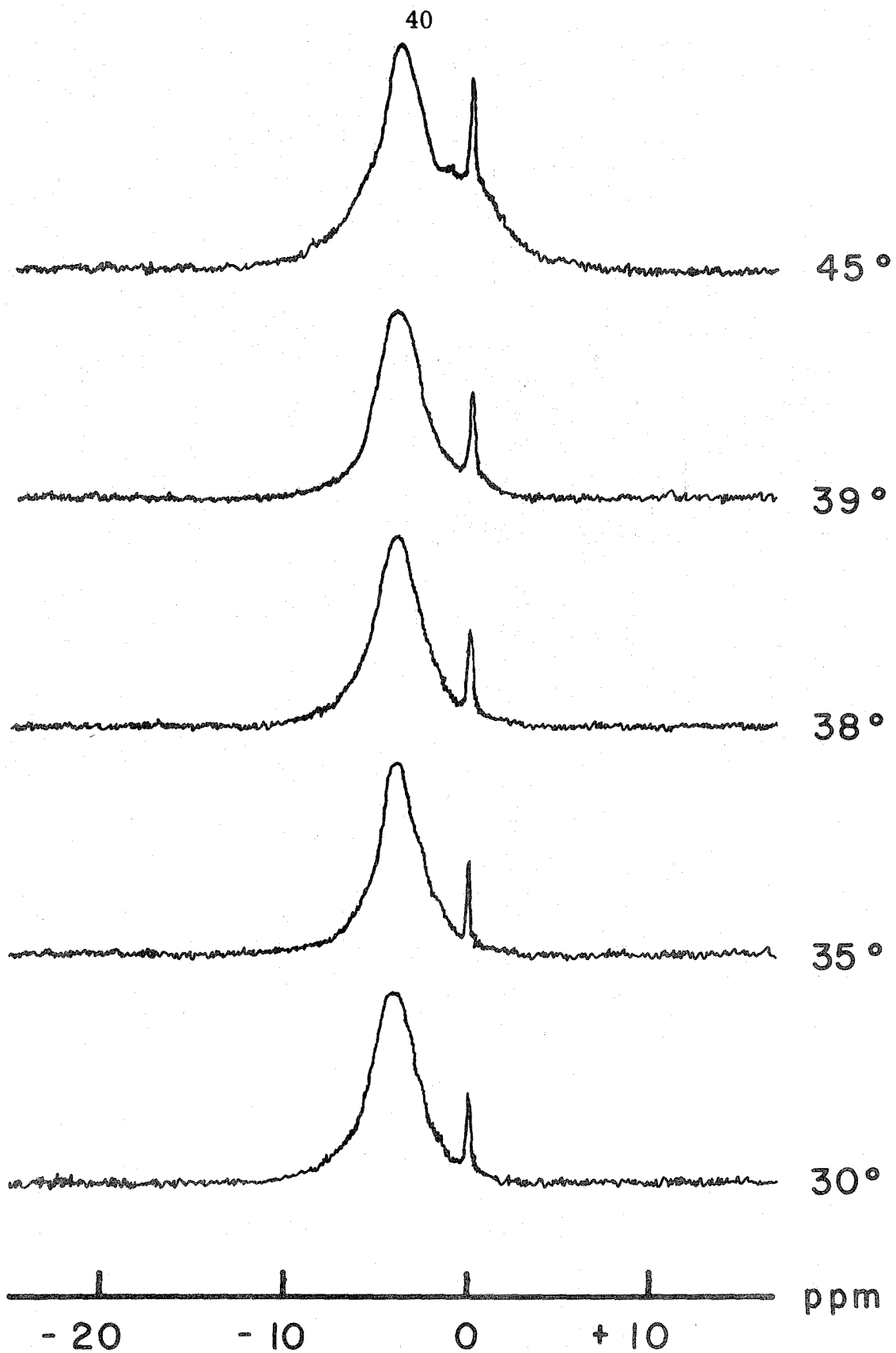


FIGURE 10

220 MHz cw proton magnetic resonance spectra of aqueous dipalmitoyl lecithin. The sample was prepared with H₂O.



an attempt to elucidate the origins of this peak. D. T. A. plots for samples of dipalmitoyl lecithin containing CaSO_4 , glutamic acid, adamantane and valinomycin are shown in Figure 11. The first three additives were used as controls for comparison with the sample containing valinomycin, which is known to interact predominantly with the polar head group region of lecithin. (67) In all of these samples, the mole ratio of lecithin to additive was 50 to 1. It can be seen that the additives have no effect on the D. T. A. plot, except for valinomycin, which entirely eliminates the pre-phase transition peak without affecting the main peak.

2. Above the phase transition temperature. The pmr spectra of dimyristoyl lecithin in the bilayer phase are shown in Figure 12 (a-c). The 51.7 and 23.5 kgauss spectra were obtained in the continuous wave mode, whereas the 14.1 kgauss spectrum is the Fourier transform of a free induction decay, with no data collection delay. The downfield spike arises from the residual protons in the D_2O . The sharp central line, about 100 Hz wide, is from the choline methyl protons. The sharp upfield line, about 200 Hz wide, has its origin in the terminal methyl protons on the lecithin side chains. The remaining protons, which are predominantly from methylene groups, appear as a spectral band several thousand Hz in width. There is clearly a field dependence of the lineshape, although the precise magnitude of the dependence cannot be readily determined. This difficulty comes about because the linewidth depends upon a

FIGURE 11

Differential thermal analysis plots for aqueous dipalmitoyl lecithin samples containing the additives (a) CaSO_4 , (b) glutamic acid, (c) adamantane, and (d) valinomycin.

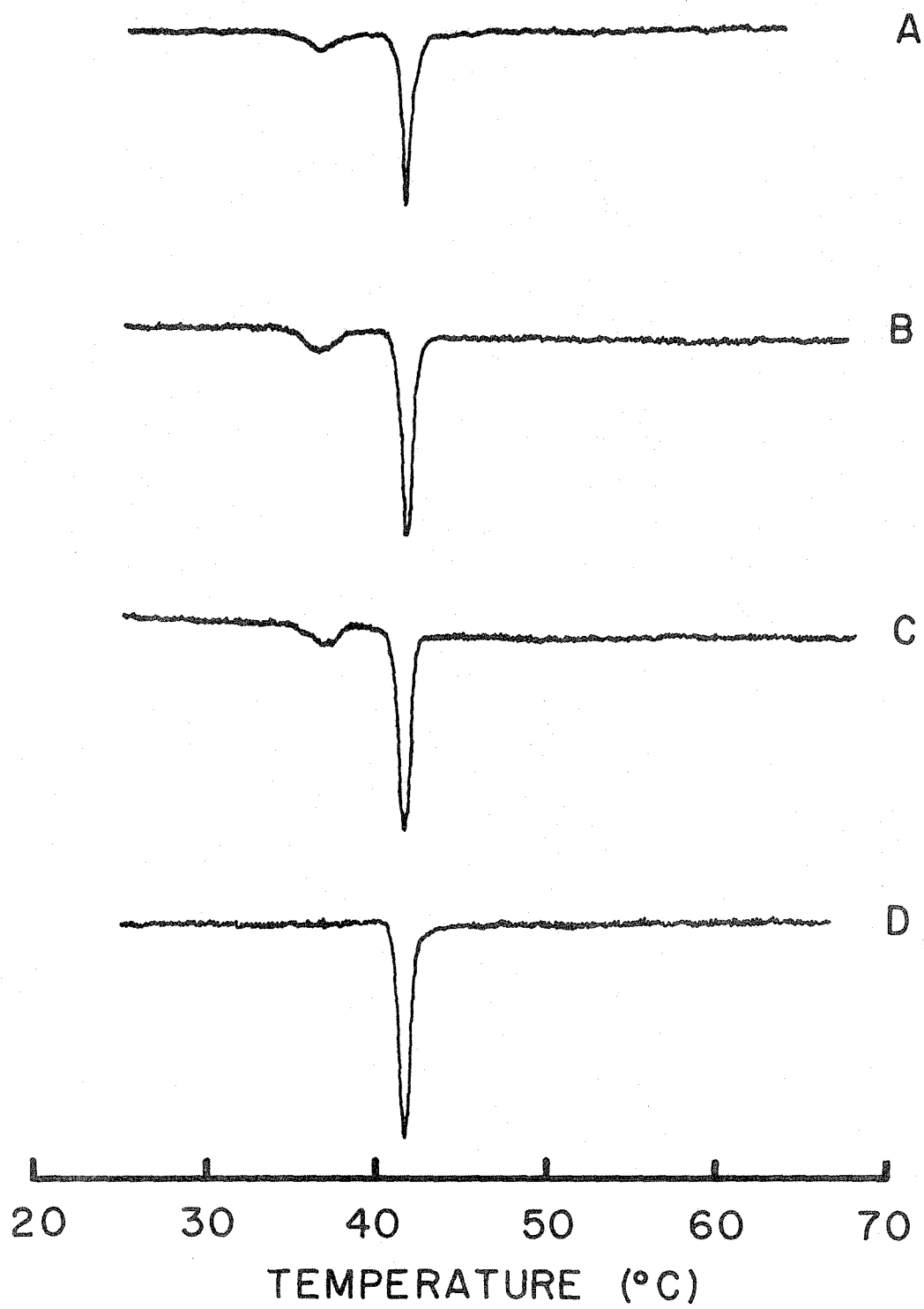
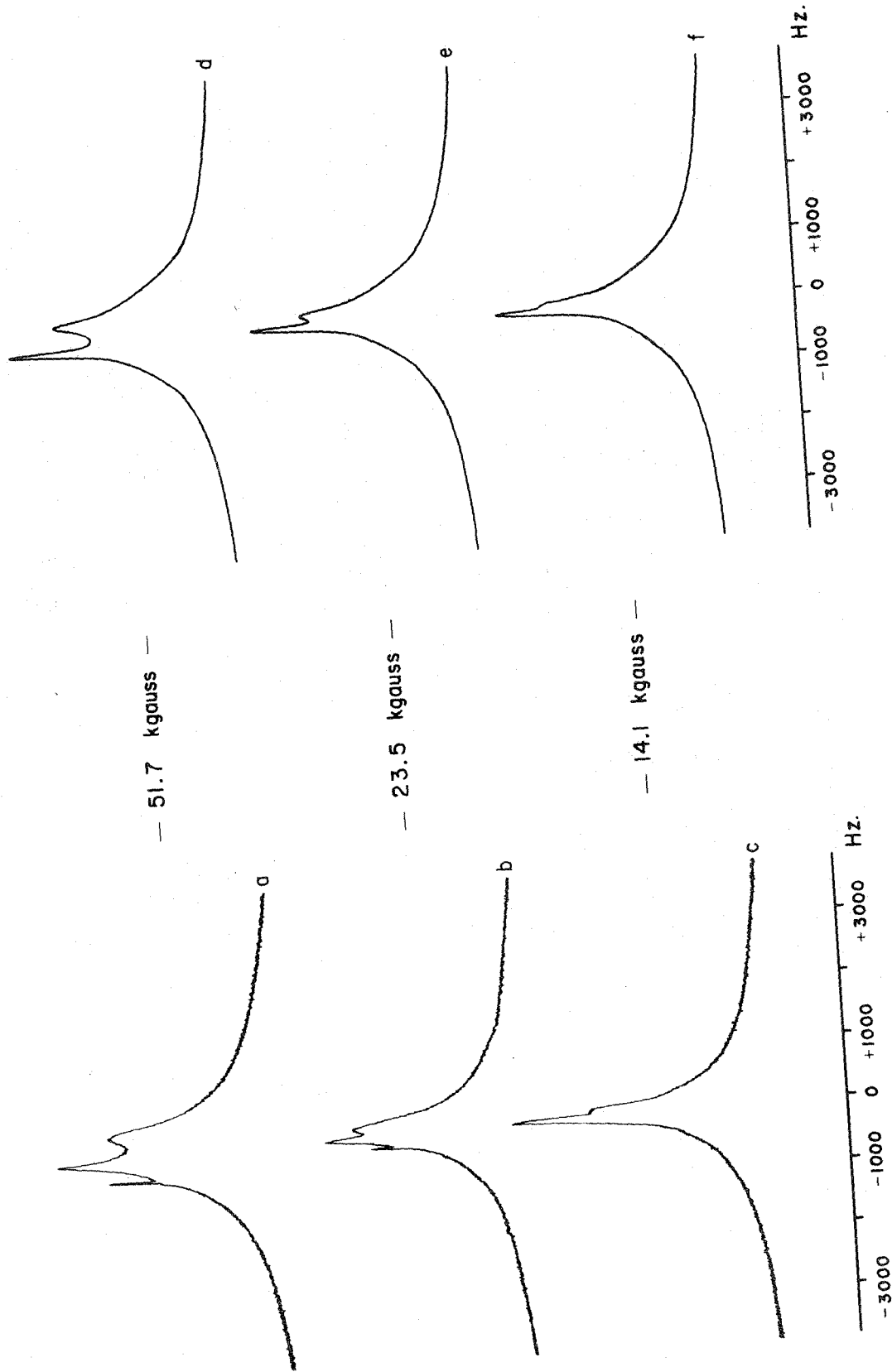


FIGURE 12

Magnetic field strength dependence of the lineshape of the pmr spectra of dimyristoyl lecithin multilayers at 30° (a, b, c) and comparison of these experimentally observed spectra with computer simulated spectra (d, e, f). The simulated spectra are composed of the sum of the following Lorentzian lines: (i) a peak 3000 Hz wide containing 75% of the total signal intensity, centered at 0.0 ppm, corresponding to the methylene protons, (ii) a peak containing 5% of the total signal intensity, 100 Hz wide, centered at -1.6 ppm, corresponding to the narrow choline methyl resonance, (iii) a peak containing 10% of the total signal intensity, 3000 Hz wide, centered at -1.6 ppm, corresponding to the broad choline methyl resonance, (iv) a peak 200 Hz wide containing 5% of the total signal intensity, centered at +0.37 ppm, corresponding to the narrow terminal methyl resonance, and (v) a peak 3000 Hz wide containing 5% of the total signal intensity, centered at +0.37 ppm, corresponding to the broad terminal methyl resonance.



choice of the peak height, which is indeterminate because of the presence of sharp peaks superimposed on a broad peak. Also, the choice of the spectral baseline is subject to considerable uncertainties.

The pmr absorption spectrum described above contains peaks from various methyl and methylene groups with significant chemical shift differences. In order to determine whether the chemical shift difference between the choline methyl, the terminal methyl, and the methylene groups could account for the observed magnetic field dependence of the lineshape, we have computer-simulated the spectra at 51.7, 23.5 and 14.1 kgauss, including the expected chemical shift between the peaks. These spectra are shown in Figure 12 (d-f).

3. Delayed Fourier Transform spectra. The spectra shown in Figure 10 contain both broad and narrow components. Linewidth and intensity measurements on the narrower resonances of these spectra are difficult, because these peaks appear superimposed against the broader resonances. It is possible, however, to filter out the broad resonances from the spectrum when using pulse nmr methods by introducing a delay time between the end of the rf pulse and the start of data collection.⁽⁶⁶⁾ Each component of the transient signal will then have decayed to $\exp(-\Delta\tau/T_2)$ of its initial value by the time the recording of the transient begins. Here $\Delta\tau$ is the length of the pulse plus the chosen delay time, and T_2 is the spin-spin relaxation time associated with a given component. The resulting Fourier transformed spectrum will then exhibit all the components

present in the usual cw nmr spectrum, but with each component weighted by its own factor $\exp(-\Delta\tau/T_2)$. The effect of this weighting process on lines of various widths is shown in Table I.

The advantage of this filtering effect may be seen by comparing the cw spectrum with the Delayed Fourier Transform (DFT) spectrum of aqueous egg lecithin bilayers, as shown in Figure 13. The cw spectrum reveals several narrow components, but the bulk of the signal is very broad and obscures the sharper resonances, making it difficult to determine their spectral position and intensity. In the DFT spectrum in Figure 13, the broad component in the cw spectrum can be seen to be essentially completely "filtered", and the narrower components can be readily monitored.

The DFT technique has enabled us to monitor the crystal \rightarrow bilayer phase transition in aqueous dipalmitoyl lecithin. As shown in Figure 14, the crystalline phase of the lecithin reveals no sharp components. Above the Kraft temperature of 41.5°C , the lecithin methyl peaks appear. The spectral intensities of the choline methyl and the terminal methyl resonances are plotted as a function of temperature in Figure 15. These intensities are presented as a percentage of the expected intensity of each chemical species, calculated from the molarity of the species in the sample. It can be seen from Figure 15 that both the choline and the terminal methyl groups are simultaneously mobilized at the bilayer phase transition temperature.

The sudden appearance of choline and terminal methyl peaks

TABLE I. Selective Filtering Effect of a Data-Collection-Delay Time $\Delta\tau = 500 \mu\text{sec}$ on NMR Lines of Various Widths in Fourier Transform NMR Spectroscopy.

<u>$1/\pi T_2$, Hz</u>	<u>Fraction of magnetization remaining</u>
10	0.98
50	0.92
100	0.85
200	0.73
500	0.46
1000	0.21
2000	0.04

FIGURE 13

High-resolution pmr spectra of aqueous lecithin bilayer samples: (a) 220 MHz cw spectrum of egg lecithin bilayers at 29°; (b) 100 MHz Delayed Fourier transform spectrum of dipalmitoyl lecithin bilayers at 60°. The peak centered at -1.14 ppm is assigned to terminal methyl groups on the hydrocarbon side chains of the lecithin molecule. The resonance at -3.32 ppm is from choline methyls of the ionic head groups. The residual protons in the solvent (D₂O) appear at -4.48 ppm. The peak at -6.42 ppm is a calibrated intensity standard of chloroform doped with the free radical, 2,2-diphenyl-1-picrylhydrazyl. Chemical shifts are referred to external TMS (10% in carbon tetrachloride).

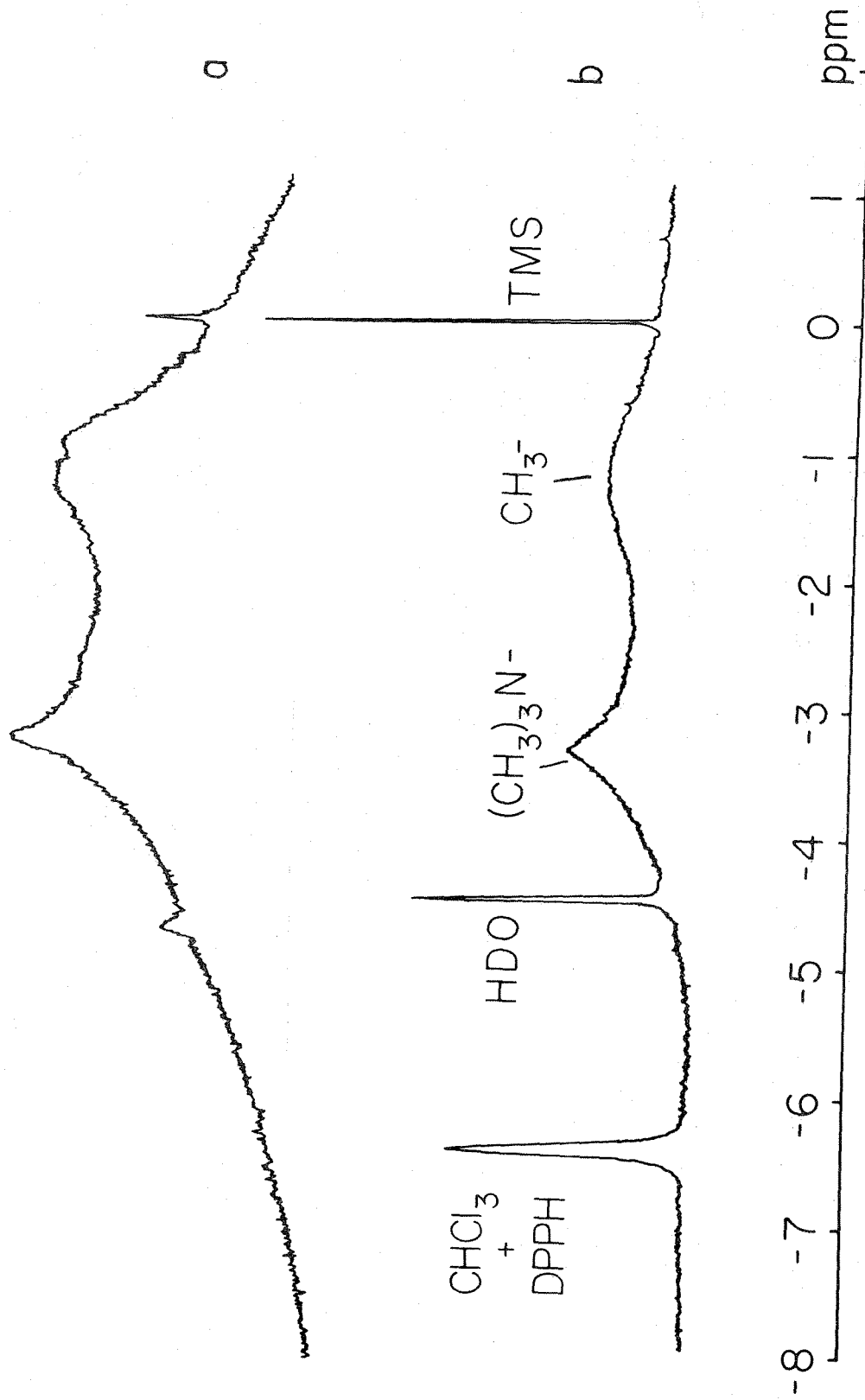


FIGURE 14

Delayed Fourier Transform pmr
spectra of aqueous dipalmitoyl
lecithin.

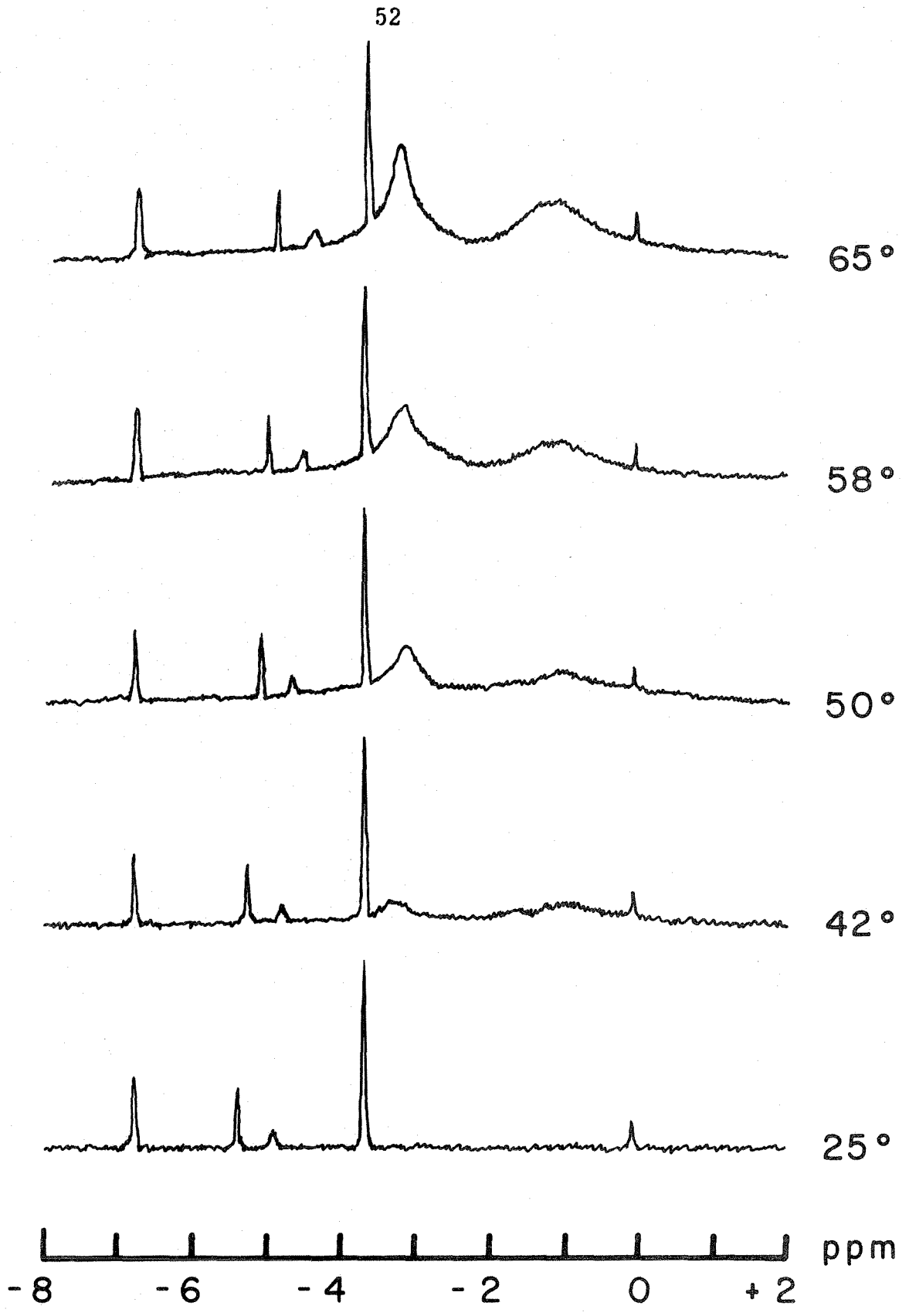
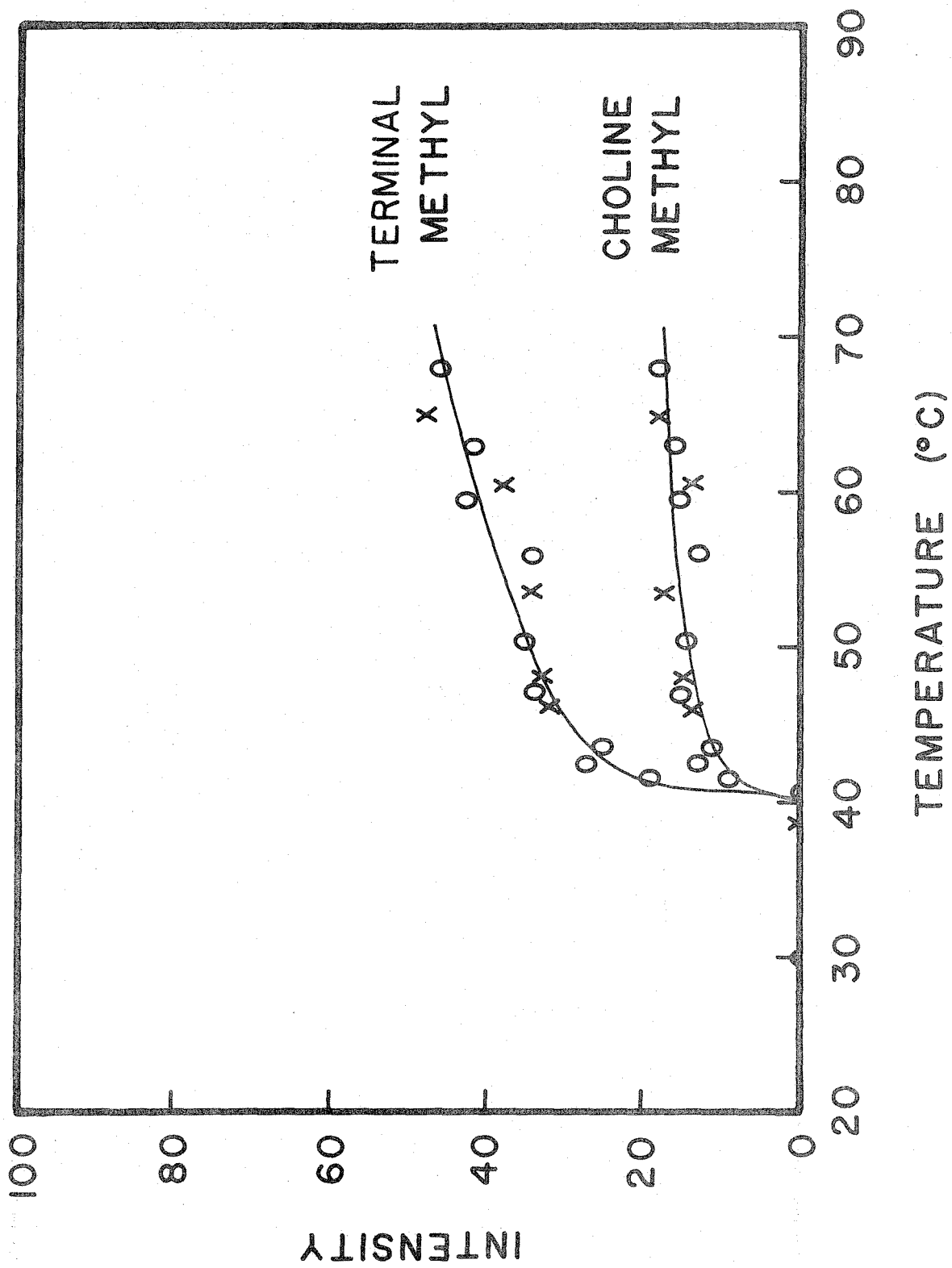


FIGURE 15

Variation of the choline and terminal methyl signal intensities with temperature for a dipalmitoyl lecithin bilayer sample, using Delayed Fourier Transform pmr at 100 MHz.



in the DFT spectra correlated exactly with the dramatic line-narrowing of the broad resonances in the 100 MHz cw spectra. The advantage of using the HA-100 spectrometer for both DFT and wide-line cw measurements was that the sample did not need to be removed from the spectrometer between DFT and cw experiments. In this way it was determined that the temperature at which the methyl peaks appeared in the high resolution DFT spectra was precisely the same temperature at which the bulk of the cw signal narrowed, i. e., the signal from the hydrocarbon chain methylene protons.

Using the DFT method, the linewidth and intensity measurements for the choline and terminal methyl signals are given in Table II for several varieties of lecithin. It is clear that significantly less than 100% of the signal from the methyl group protons appears with the linewidth indicated in the high resolution spectrum.

The DFT method enables us to determine the T_1 values of the individual methyl resonances, since these resonances become isolated from the bulk of the signal and are thereby sufficiently distinct from each other. T_1 was determined from the magnetization recovery following a 180° - 90° pulse sequence, and Fourier transforming the free induction decay after the 90° pulse. The magnetization recovery for choline and terminal methyl resonances is shown in Figure 16. The recovery is exponential, indicating the presence of only one value of T_1 . The T_1 values at several temperatures and at 51.7 and 23.5 kgauss are given in Table III.

TABLE II. Linewidth and Intensity Results
for DFT Experiments

<u>Lecithin</u>	<u>Methyl Group</u>	<u>% of Protons Observed</u>	<u>Linewidth (Hz)</u>
Egg yolk ^a	Choline	30	100
	Terminal	60	150
Dipalmitoyl ^b	Choline	30	110
	Terminal	50	180
Dimyristoyl ^a	Choline	20	110
	Terminal	40	180

^a At 30°C.

^b At 50°C.

FIGURE 16

Recovery of the magnetization for
choline methyl and terminal methyl
protons of a dimyristoyl lecithin
multilayer sample after a 180° pulse
at 30° for magnetic fields of 51.7 and
23.5 kgauss.

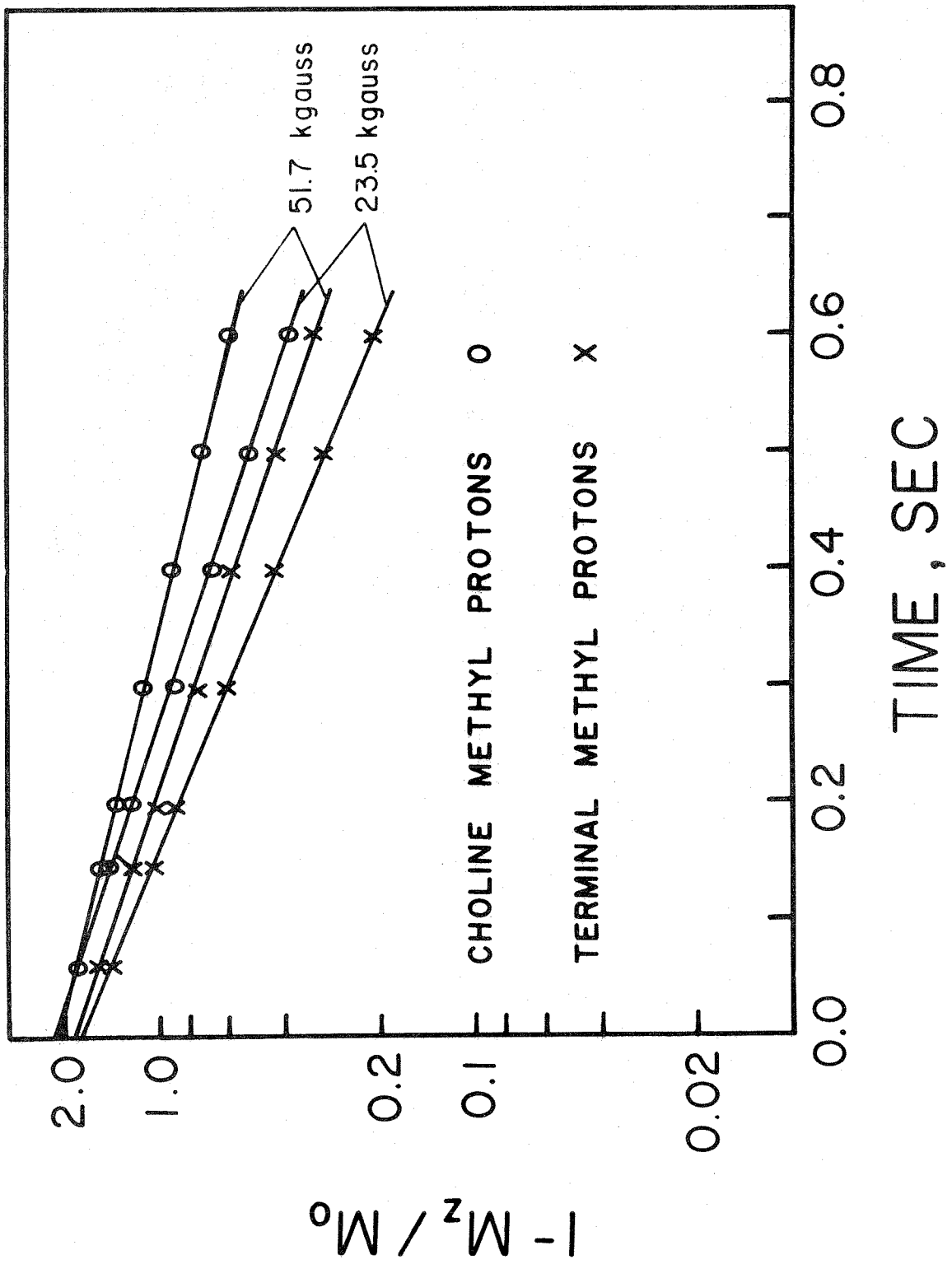


TABLE III. Temperature and Magnetic Field
Dependence of the Spin Lattice
Relaxation Times (sec) for the
Methyl Protons of Dimyristoyl
Lecithin Multilayers

<u>Temp, °C</u>	51.7 kgauss		23.5 kgauss	
	<u>Choline</u>	<u>Terminal</u>	<u>Choline</u>	<u>Terminal</u>
30°	0.37	0.33	0.29	0.26
39°	0.40	0.39	0.40	0.31
61°	0.47	0.47	0.48	0.44
75°	0.66	0.55	0.50	0.48

4. T₂. In order to examine the magnetic field strength dependence of the spin-spin relaxation time, the proton free induction decay for dimyristoyl lecithin bilayers was measured at 14.1, 12.7 and 5.16 kgauss, and T₂ computed as the time for decay of the signal to 1/e of the initial value. The free induction decay was not obtained at higher magnetic fields because the high-field instruments, designed for studies of small molecules in solution, severely distort the initial (100-200 μsec) part of the free induction signal. The T₂ data obtained at the lower fields are given in Table IV. There is no magnetic field dependence evident in these data.

The temperature dependence of the free induction decay at 12.7 kgauss for an entire sample of aqueous dipalmitoyl lecithin was studied for the purpose of comparing the temperature dependent change in this measurement with the observed pmr linewidth change at the Kraft temperature. The free induction decay for this sample is shown just below and just above the Kraft temperature of 41.5°C in Figure 17. Because of the receiver deadtime of ~ 20 μsec, the free induction decay at the lower temperature does not give an accurate measure of T₂. The free induction decay above 41.5°C falls to 1/e of its initial value in 120 μsec, which is taken as the value of T₂.

5. T₁. The magnetization recovery for the protons of an entire multilayer sample following a 180°-90° pulse sequence is shown at three different magnetic field strengths in Figure 18.

TABLE IV. Magnetic Field Dependence of Line-
widths and Transverse Relaxation
Rates at 30°C

<u>Magnetic field (kgauss)</u>	<u>Apparent linewidth</u>	<u>Observed T₂ (μsec)</u>	<u>1/π T₂ (Hz)</u>
51.7 ^a	1700	-	-
23.5 ^a	1100	-	-
14.1 ^a	850	135	2360
12.7 ^b	-	120	2650
5.16 ^b	-	125	2550

^a Dimyristoyl lecithin multilayers.

^b Egg yolk lecithin multilayers.

FIGURE 17

The proton free induction decay
of an aqueous dipalmitoyl lecithin
sample in a magnetic field of 12.7
kgauss at (a) 28°C and (b) 42°C.

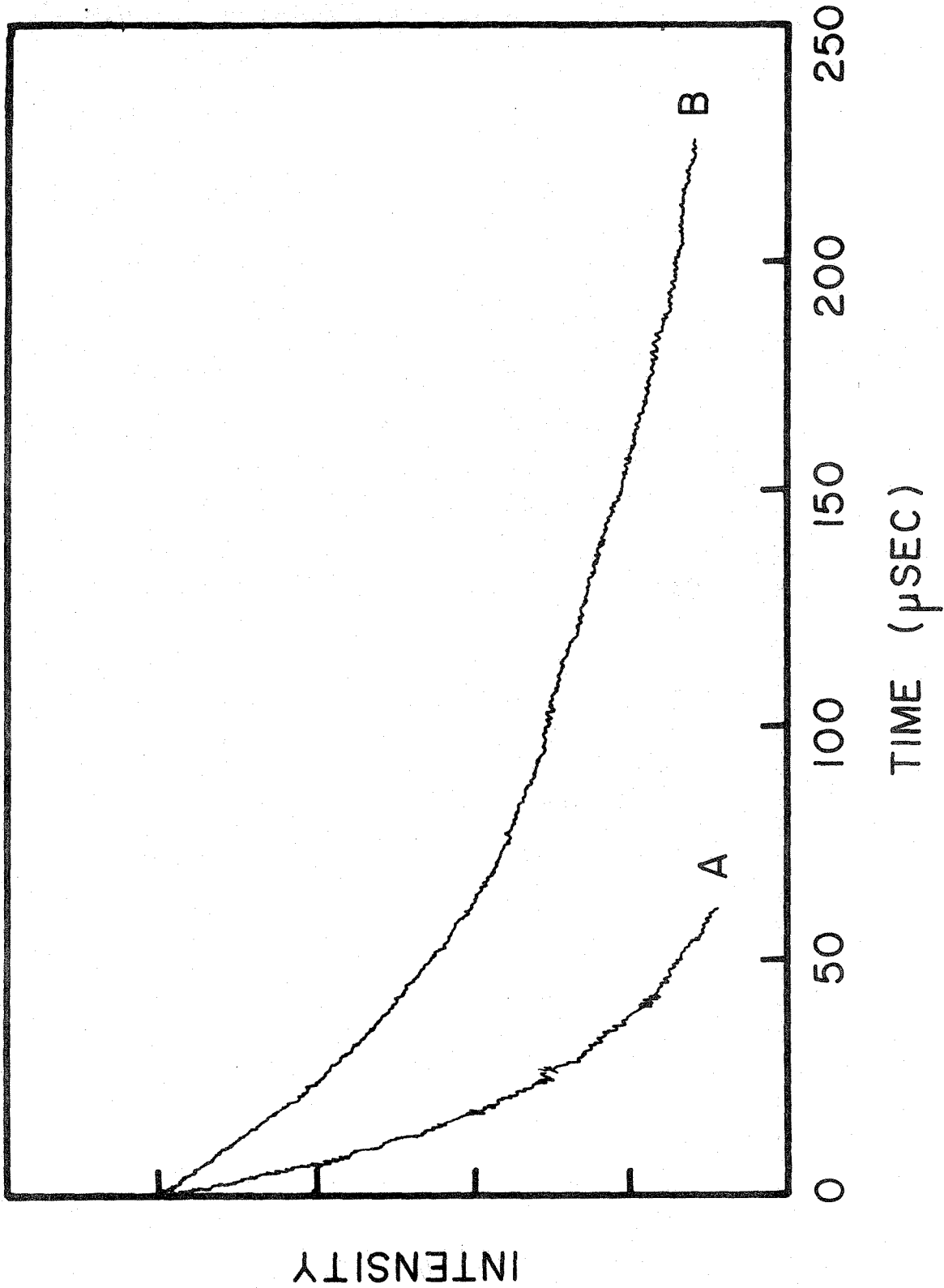
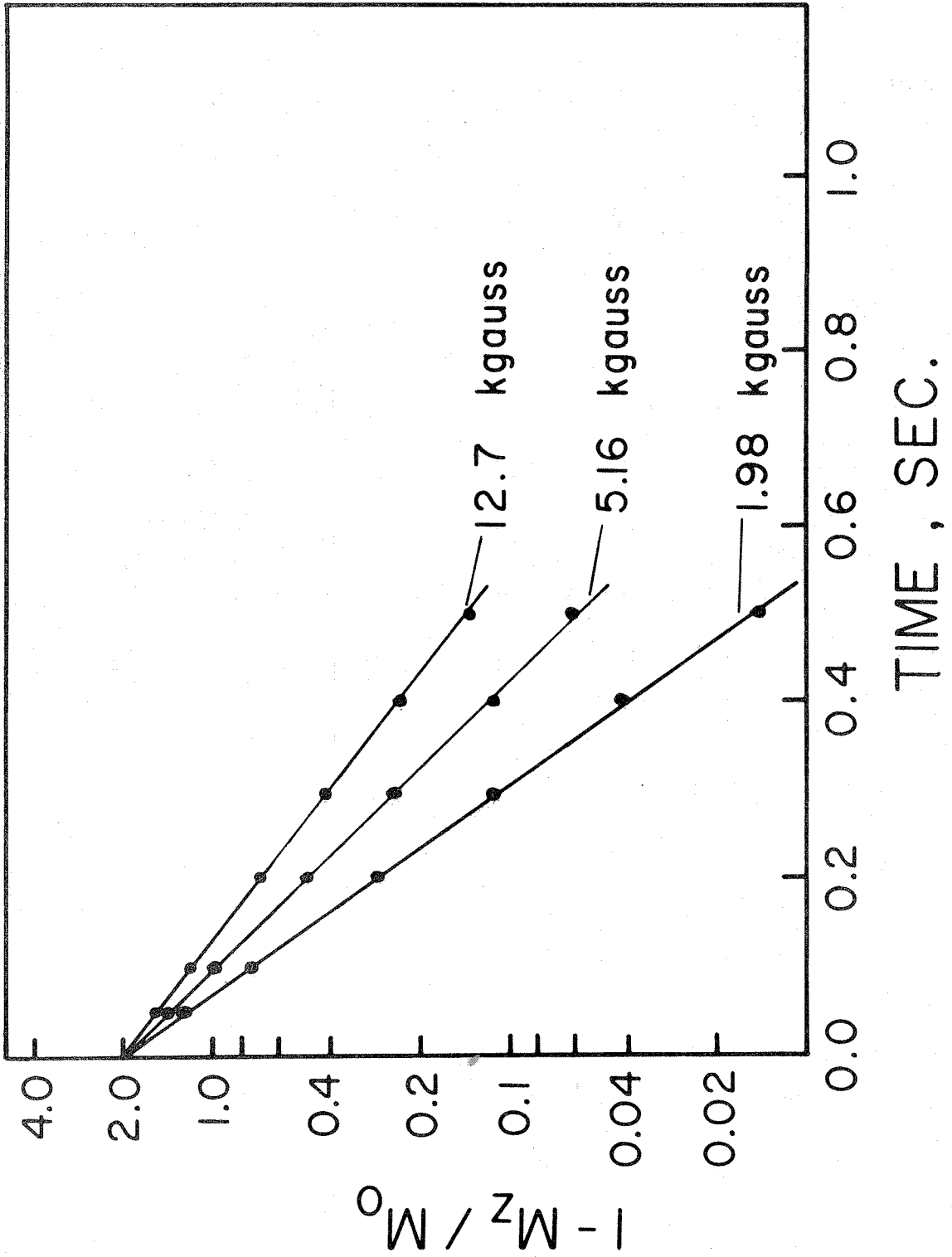


FIGURE 18

Recovery of the magnetization of all of the protons in an egg yolk lecithin multilayer sample after a 180° pulse at 30° for three different magnetic field strengths.



This magnetization recovery is exponential, indicating one value for T_1 . The temperature dependence of the T_1 values at each field is given in Figure 19.

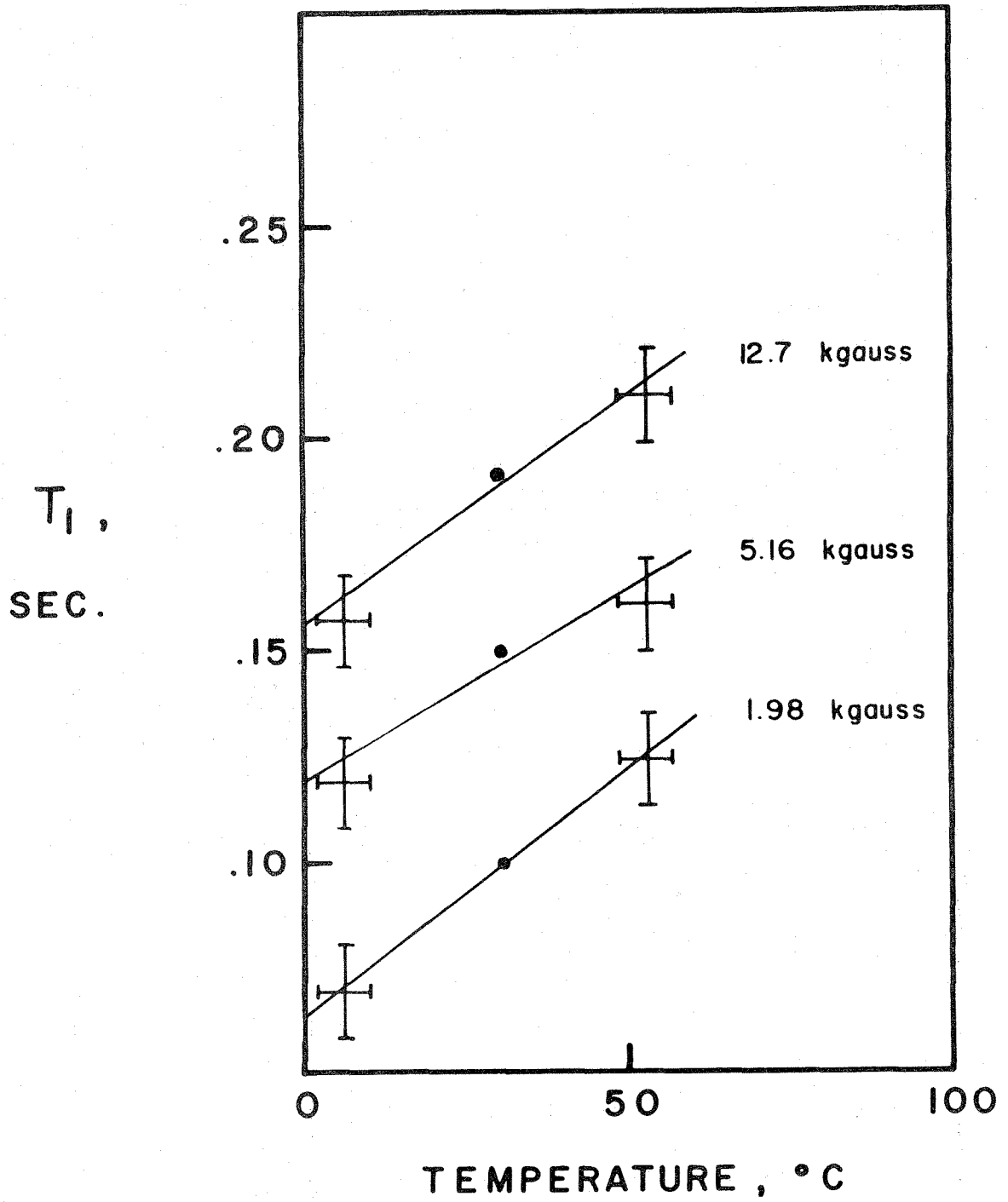
V. Discussion

1. Field-dependent lineshape. From Figure 12 it is clear that the entirety of the field dependence of the linewidth can be accounted for by the chemical shift differences of the protons since the chemical shift is a necessary and sufficient line-broadening mechanism. Therefore, an additional field-dependent line broadening effect is not called for. It was possible to reproduce the shape of the experimentally observed spectra with broad components comprising the bulk of the signal, choline and terminal methyl signals which appear with less than 100% of their intensity in narrow signals, and choline and terminal methyl components of greater linewidths comprising the remainder of these signals. We point out that the principal feature of the computer simulated spectra, i. e., the field-dependent linewidth, is not sensitive to details of the composition of the line. We find a similar field dependence with many different simulated compositions, as long as a chemical shift difference is included in the simulated spectra.

An important aspect of the linewidths determined from the continuous wave spectra is that they are not at all in agreement with the values of $1/\pi T_2$, obtained from the free induction decay

FIGURE 19

Temperature dependence of the proton spin-lattice relaxation time for a bulk sample of egg yolk lecithin multilayers for magnetic field strengths of 12.7, 5.16 and 1.98 kgauss.



after a 90° pulse. This is especially apparent at 60 MHz where both the free induction decay and the Fourier transform of that free induction decay were available. This fact should not be surprising, since the relationship between the linewidth and T_2 computed from the $1/e$ value of the free induction decay is not known a priori for a complex lineshape. When the lineshape is given by a simple mathematical function, T_2 is related to the linewidth in a simple way. The two known examples of such simple relations are the Lorentzian lineshape, for which

$$\Delta\nu = \frac{1}{\pi T_2}$$

and the Gaussian lineshape, for which

$$\Delta\nu = \left(\frac{\ln 2}{\pi}\right)^{\frac{1}{2}} \frac{1}{T_2}$$

where $\Delta\nu$ corresponds to the linewidth measured at half maximum intensity. In the case of the lecithin molecule, not only are appreciable intensities of chemically shifted species present, but also the individual resonance from each component cannot be presumed to be of a simple shape, since the molecule may be undergoing anisotropic and restricted motion.⁽³²⁾ Moreover, the presence of narrow lines in the observed continuous wave spectrum gives disproportionate weight to these lines when the width at half height is determined. On the contrary, the initial height of the free induction decay after a 90° pulse contains each component weighted

simply by its actual intensity, and, in time, each component of the free induction decay decays with its own value of T_2 . If one component of the free induction decay is dominant in intensity, then the overall T_2 is largely determined by this one component. This is the case for the lecithin studied here wherein the methylene protons make up over 70% of the signal.

In summary, the linewidth is not a meaningful measure of spin-spin relaxation for a complex spin system. The T_2 determined from the free induction decay is a reliable measure of the spin-spin relaxation, even for a complex system. In contrast to the apparent linewidth, T_2 is independent of magnetic field strength for lecithin multilayers.

The appearance in the pmr spectrum of less than 100% of the expected intensity for the methyl resonances has been interpreted to indicate solid-like features of the methyl spectrum.⁽³²⁾ The unseen intensity is not contained in other resonances, such as from methyl protons which are in a different motional state or at an unpropitious angle to the magnetic field. Rather, the signal which does show up with the indicated linewidth arises from a particular set of energy transitions, and contains contributions from all protons from the particular chemical species of methyl group. We point this out because we later use T_1 values from the observed methyl resonances to establish a motional model for the entire system of methyl protons.

It is appropriate at this point to comment on the Carr-Purcell

results, ⁽⁶¹⁾ which have been interpreted to indicate that molecular diffusion through magnetic field gradients is an important cause of the spectral linewidth. Because of the time scale on which these pulse sequence measurements were made, it is clear that the greater part of the free induction decay in these experiments would be lost by the time of the first Carr-Purcell pulse, and thus only the tail of the decay could contribute to the echo signal. This can be understood by examination of Figure 17, which shows that after waiting 100-1000 μ sec, a typical range of the time between pulses in the Carr-Purcell sequence, most of the signal from lecithin bilayers is lost. These Carr-Purcell results therefore do not provide insight into the dominant relaxation mechanism.

2. Molecular mobility at the Kraft temperature. From the wide-line 100 MHz cw spectra and the 100 MHz DFT spectra, it is clear that the hydrocarbon side chains, the choline head group methyls, and the terminal methyls on the hydrocarbon side chains of the dipalmitoyl lecithin molecule are all simultaneously mobilized at 41°C. The change from a very fast free induction decay below 41°C to a free induction decay with a T_2 of 120 μ sec above 41°C, observed at 54 MHz on the pulse nmr equipment, confirms that the protons giving rise to the bulk of the proton magnetic resonance signal, i. e., the hydrocarbon side chain methylene protons, undergo a mobility increase at the Kraft temperature. This temperature corresponds precisely to the main peak in the D. T. A.

plot. Scrutiny of the DFT spectra in Figure 14 reveals no trace of a high resolution pmr signal from the lecithin below 41°C. Only at 41°C are all parts of the lecithin molecule mobilized. Since the temperature of the nmr probe could be varied and measured only in relatively coarse gradations of 0.5°-1.0°C or more, it is conceivable that there could be undetected mobility of some part of the lecithin molecule just prior to the mobilization of the rest of the molecule. This latter possibility is not considered to be likely, because it was found reproducibly that choline and terminal methyl resonances appeared simultaneously in the DFT spectra.

3. Molecular motion in the crystal phase of lecithin. The change in the pmr spectrum which was used to monitor molecular mobility is sensitive only to frequencies of molecular motion in excess of 10^6 sec^{-1} . The onset of any slower motion would not be detected in these experiments as a line-narrowing. Such slower motions could be monitored by measurements of $T_{1\rho}$, the relaxation time in the field of the irradiating radiofrequency. (68) $T_{1\rho}$ measurements are sensitive to frequencies of approximately 10^3 to 10^7 sec^{-1} . However, in order that the irradiating field be sufficiently strong to cover the range of local magnetic fields within the sample, the irradiating field must be ≥ 10 gauss, limiting the $T_{1\rho}$ technique to frequencies of 10^5 to 10^7 sec^{-1} . A motional change at a lower frequency than this could perhaps be monitored by ultrasonic or dielectric relaxation. However, we expect the pmr method used

in this study to be sufficient for detecting the onset of molecular motions corresponding to the formation of the liquid crystal (bi-layer) from the crystal. This conclusion comes from the interpretation of Figure 8a, which shows that even in the crystal state there is significant molecular motion, enough to narrow the pmr signal of some part of the lecithin molecule to 2400 Hz. This means that some part of the lecithin molecule must be moving with a frequency of at least $\sim 10^7 \text{ sec}^{-1}$, in the crystal state. Thus we might reasonably expect that increases in molecular motion over the crystal state value would show up as an observable narrowing of the pmr signal.

The assignment of the broad and the narrow resonances of the pmr spectrum of lecithin in the crystal state is not straightforward. Vekslı et al., (39) using conventional wide-line pmr equipment, found for aqueous dipalmitoyl lecithin below the Kraft temperature a broad component of linewidth approximately 5 gauss (22,000 Hz) and a narrower component about 0.4 gauss (1700 Hz) in width. The narrower component was assigned to the choline methyl protons on the basis of signal intensity measurements of dipalmitoyl lecithin with deuterated side chains. For an undeuterated sample, the narrow resonance should account for 12% of the total lecithin pmr signal if it arises solely from the choline methyl protons. However, our intensity measurements show this narrow line to account for approximately 25% of the total pmr signal. It is possible that the pmr lineshapes of lecithin below the Kraft

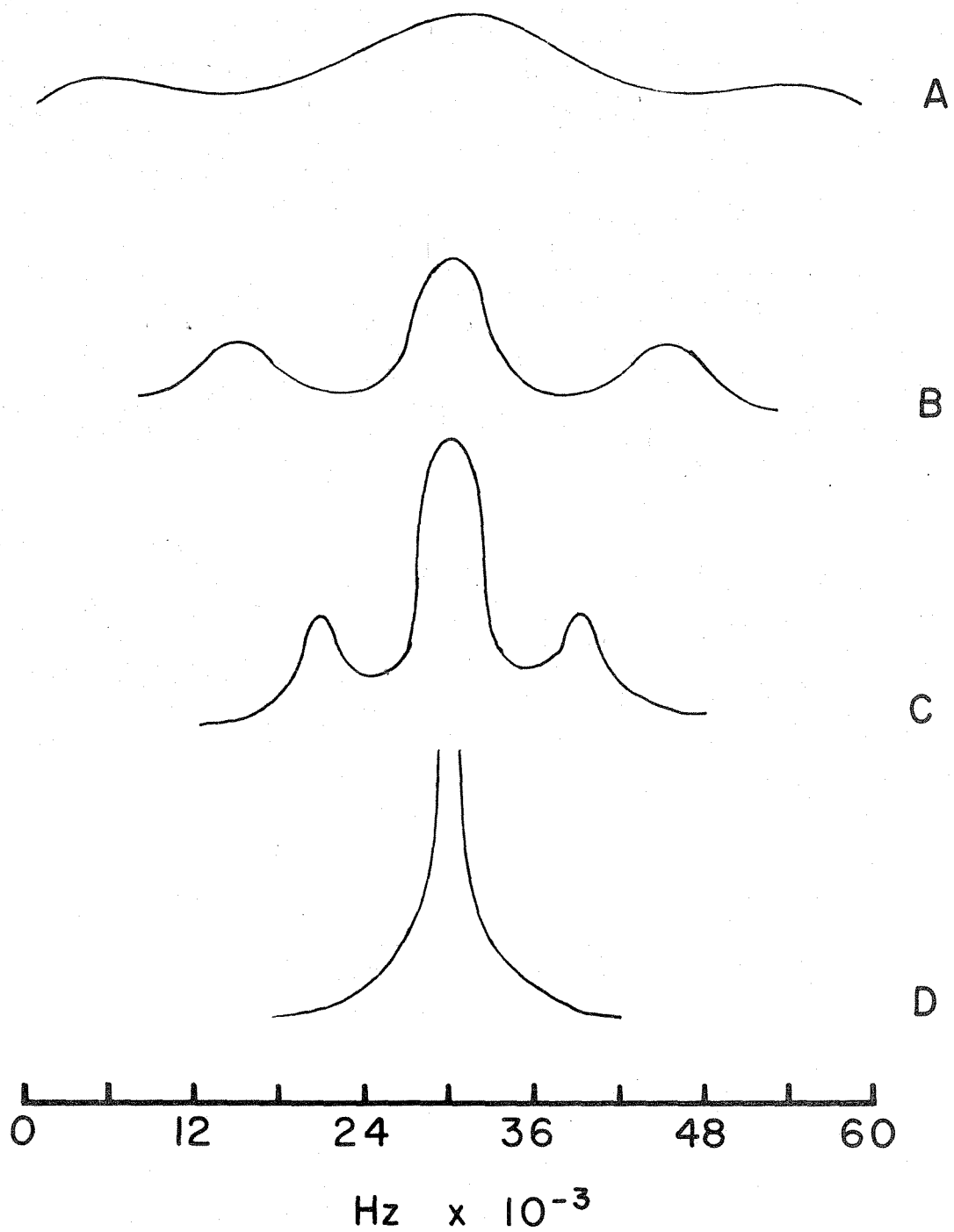
temperature are sufficiently unusual that the choice of a baseline for the narrow component is in error, and the observed intensity really is 12%. On the other hand, if our value of 25% is approximately correct, then other protons of the lecithin, in addition to the choline methyl protons, must be sufficiently mobile to appear in a pmr signal 2400 Hz in width. The likely candidates for these mobile protons would be the terminal methyl protons, together with some methylene protons, perhaps those near the methyl end of the lecithin hydrocarbon side chains.

The motion of methyl groups at the temperatures at which these experiments were conducted certainly includes a rapid, i. e., 10^9 - 10^{11} sec⁻¹, reorientation about the methyl rotor axis. (32, 63) The effect of this motion on the pmr spectrum of methyl protons is shown in Figure 20. From this figure it can be seen that very little of the signal intensity would appear in the narrow (2400 Hz) resonance of aqueous dipalmitoyl lecithin in the crystal state. In order that the entirety of the methyl pmr signal appear as a single resonance of \sim 2400 Hz in linewidth, considerable off-axis motion of the methyl group would be required, in addition to the rapid reorientation about the rotor axis. Using the method developed by Seiter and Chan for treating anisotropic motion, (32) it can be shown that the methyl rotor must undergo excursions of at least 50° off-axis. Furthermore, because the methyl rotor axis orientation is determined by the covalent bond to the neighboring methylene group, it is expected that there should also be significant motion of this

FIGURE 20

The effect of motion on the pmr spectrum of the methyl three-spin system.

- (A) no motion.
- (B) rapid reorientation about the methyl rotor axis. No off-axis motion.
- (C) rapid reorientation about the methyl rotor axis, together with off-axis excursions of $\Delta\theta' \approx 40^\circ$.
- (D) rapid reorientation about the methyl rotor axis, together with off-axis excursions of $\Delta\theta' \approx 70^\circ$.



methylene group, and therefore a methylene contribution to the narrow pmr signal.

Similar considerations for the choline methyl groups imply that these also undergo off-axis excursions of at least 50° , in addition to rapid reorientation about the rotor axis, in order that the entirety of the choline methyl pmr signal appear as a line ~ 2400 Hz wide.

We may examine the other possibility about the origin of the narrow resonance, namely that it does not contain a contribution from the "wings" of the methyl spectrum, as shown in Figure 20, but only from the central resonance. If this is so, and if the 2400 Hz wide peak actually does account for $\sim 25\%$ of the total lecithin pmr signal, then the remainder of the observed intensity of this narrow peak must come from the equivalent of approximately 20 protons from somewhere in the dipalmitoyl lecithin molecule. However, if the terminal methyl group is undergoing such small off-axis excursions that it does not fully contribute to the 2400 Hz wide resonance, then it is hardly possible that methylene protons farther up the hydrocarbon side chains could be more mobile. This reductio ad absurdum argument shows that there must be significant mobility of choline and terminal methyl groups, and perhaps of some methylene groups, even in the crystalline state of lecithin.

4. Methyl groups above the Kraft temperature. The progress of the crystal to liquid crystal phase transition can be followed by the

DFT pmr spectrum of the choline and the terminal methyl resonances. The phase transition plot of Figure 15 has several interesting features. Both ends of the lecithin molecule become mobile simultaneously. The intensity observed, up to 70°C, does not approach 100% of the expected intensity. This perhaps unexpected result can be explained by referring to Figure 20, the calculated spectra for a methyl three-spin group under various conditions. It can be seen that when the intermolecular contribution to line broadening is sufficiently small, and when the extent of off-axis motion of the methyl rotor is less than about 80°, much of the signal appears in a broad line which is quite distinct from the central peak. The broad part of the resonance is filtered out by the DFT technique, and disappears in the spectral baseline. Thus, we conclude that at least up to 70°C, the motion of the choline methyl and the terminal methyl groups in the bilayer phase is not isotropic and is highly restricted.

The pmr signal intensities shown in Figure 14, which were used to monitor the progress of the phase transition, contain both heating and cooling points. This experiment was conducted by heating the sample, equilibrating for 1/2-3/4 hour at each temperature and recording the spectrum. When the maximum temperature was reached, the sample was then cooled, again equilibrating for 1 3/4 hour at each temperature before recording the spectrum. There is no evidence of hysteresis.

5. Comparison of pmr and D. T. A. results. The series of 220 MHz spectra at various temperatures shown in Figure 9 was used to closely examine the pmr lineshape of lecithin below the Kraft temperature. In particular, we wanted to determine whether there was a change in the pmr spectrum which corresponded to the pre-phase transition peak in the D. T. A. plot, shown in Figure 5. In this way, it was hoped to identify the D. T. A. peak as corresponding to the onset of a particular sort of motion of the lecithin molecule.

These spectra show a gradual line narrowing from approximately 2500 Hz at 33°C to 1800 Hz at 41°C. However, the actual linewidth is not possible to measure, or even compare quantitatively, because the sweep width used (20,000 Hz was the instrumental maximum) was too small to define the baseline. Still, it is apparent that the intensity of the peak is increasing significantly from 33° to 41°C. Since this peak corresponds to the "narrow" resonance in the 100 MHz wide-line cw spectrum, which was assigned to choline methyl, terminal methyl, and some methylene protons, we conclude that the mobility of some methylene protons increases significantly over this temperature range, because methyl groups may be already showing up with full intensity. No abrupt change in linewidth or intensity occurs which could correlate with the D. T. A. peak from 35°-38°C.

The 220 MHz pmr spectra of a dipalmitoyl lecithin sample containing 25% H₂O by weight is shown in Figure 10. This quantity

of water corresponds to approximately 13 water molecules per lecithin molecule. The linewidth of this water does not perceptibly change from 490 ± 10 Hz between 30° and 39°C . This constancy of the linewidth indicates that either a very small change in the motional state of the water occurs, or else a larger change occurs which is in the frequency range $0-10^7 \text{ sec}^{-1}$.

The D. T. A. experiment shown in Figure 11, in which valinomycin abolishes the pre-phase transition peak, indicates that this peak is associated with a change in the vicinity of the lecithin polar head group, since this is the region in which the valinomycin is located. (67) However, the above nmr experiments indicate that any motional change which occurs is either of small magnitude or of low frequency. In other words, it is reasonable to conclude that the small D. T. A. peak corresponds to a structural rearrangement in the lecithin head group or its bound water, rather than a mobility increase.

6. The question of spin-diffusion. An important experimental quantity to interpret is the value of T_1 for the entire sample. The initial part of the proton free induction decay for the entire multilayer sample contains proportionate contributions from all of the protons in the sample, but may be considered to arise principally from the hydrocarbon chain methylene protons, since these account for about 70% of the protons in the lecithin molecule. These methylene protons would be expected a priori to be heterogeneous

their T_1 relaxation because of mobility differences among the various methylene groups along the hydrocarbon chains. However, we must first determine whether this measured T_1 value is a composition of T_1 values from the different methylene protons, or if the measured T_1 is controlled by just a small fraction of the protons.

The former case, that individual protons have their own characteristic T_1 , is the usual case in high resolution pmr. However, the latter possibility, that a specific few spins control the T_1 process for the entire spin system, occurs commonly in solids. Historically, the first example of this phenomenon was described by Bloembergen for crystals of alum, $KAl(SO_4)_2 \cdot 12H_2O$.⁽⁶⁹⁾ The immobility of the protons in this solid implies a longer T_1 than the value observed. Bloembergen showed that the spin-lattice relaxation was controlled by a very small percentage of a paramagnetic impurity. The mechanism for the relaxation originates in the weak coupling of the proton spins to the lattice, whereas the spins are strongly coupled to each other. The term "spin diffusion" was used to describe the diffusion of spin energy, via the magnetic dipolar coupling between the spins, from the entire spin system to the small number of proton spins near paramagnetic ions, which act as the heat sinks. The criterion for spin diffusion is that $T_2 \ll T_1$, together with the presence of some spins with relatively short T_1 values.

A second example of spin diffusion, somewhat more allied to our system of lecithin multilayers, is found in solid alkanes.

Anderson and Slichter⁽⁷⁰⁾ showed that the reorienting methyl groups acted as the heat sinks for the entire proton spin system because of their rapid reorientation. It should be noted that the measured T_1 value did not correspond in magnitude to the T_1 calculated for an isolated methyl group. Instead, since the methyl protons relax the entire spin system, the measured T_1 is longer than the T_1 of the protons of an isolated methyl group by a factor of the ratio of the total number of protons in the spin system to the number of methyl protons.

We must determine whether or not spin diffusion is occurring in the proton spin system of lecithin multilayers. There may be spin exchange between the terminal methyl and methylene protons, along the methylene chain, and between the choline methyl and methylene protons. Resolving the first possibility will determine whether the T_1 measured for the terminal methyl group is the intrinsic T_1 of these protons, or if the methyl group relaxation behavior is modified by coupling to methylene protons. The second possibility implicitly questions whether there is a motional difference among the methylene groups, with some fraction of the total relaxing the rest, or whether all of the chain methylene groups are in similar motional states for effecting T_1 relaxation. With regard to the last possibility, we note that the choline methyl T_1 behavior is not expected to be greatly modified by spin diffusion, since the nine choline methyl protons could be coupled to only four methylene protons, and the T_1 measured for the choline methyls

would merely be increased by 35% even in the limit of infinitely fast spin diffusion. (70)

Abragam has shown how the spin exchange rate (W) can be estimated for a solid from the second moment. (71) We shall extend this method of estimating the spin exchange rate to the case of lecithin multilayers, wherein some motional narrowing of the linewidth occurs. We assume that the lineshapes are Gaussian, so that we can replace the second moment by the square of the measured linewidth at half height. In order to calculate the spin exchange rate, it is necessary to determine the contribution to the linewidth from the particular set of spin-exchanging protons. The principal contribution to the observed linewidth is from the intra-pair (geminal) protons, whereas we seek the lesser contribution from the more distant spin-exchanging protons of interest. Accordingly, if r_1 is the distance between the geminal protons (1.79 Å for methylene protons), and if r_2 is the distance between the spin-exchanging protons (2.48 Å for a methylene proton to the nearest proton on either the next methylene group or the methylene group two bonds away; 2.66 Å for the average distance from a reorienting methyl proton to the nearest methylene proton), then W can be estimated from $\Delta\omega$, the linewidth in radians sec^{-1} determined from the free induction decay ($\approx 15,000 \text{ rad sec}^{-1}$ for lecithin multilayers), as follows:

$$W \approx \frac{\Delta\omega}{30} \left(\frac{r_1}{r_2} \right)^6 .$$

This expression predicts an exchange rate of $\approx 120 \text{ sec}^{-1}$ between nearest methylene groups, and also between the methylene groups which are two bonds away, if the hydrocarbon chain is in the all-trans configuration.

The above calculation is applicable to spin exchange among magnetic nuclei with perfectly overlapping resonances. For chemically shifted spins, and for spins with grossly different lineshapes, the spin exchange rate is less than it would be when spectral overlap is perfect. Following Abragam,⁽⁷¹⁾ this imperfect spectral overlap can be taken into consideration by multiplying W , calculated above, by the appropriate overlap integral. For example, the methyl resonance lineshape, for lecithin multilayers, is composed of a broad resonance approximately 3000 Hz in width, comprising 50% of the signal intensity and arising from one class of transitions, and a superimposed narrow resonance about 200 Hz in width, comprising the other 50% of the signal and arising from a different class of transitions.^(32, 42) Spin exchange can occur when there is a simultaneous energy conserving transition among the methylene energy levels and among either class of methyl energy levels. However, because of differences in spectral overlap, there is a large difference in the value of W calculated for the two classes of methyl energy levels. Taking into account the number of different spin exchange transitions which are possible between an interacting methylene pair of spins and a methyl three spin system, together with the estimated overlap integrals, the

overall spin exchange rate between methylene and methyl protons can be estimated to be $\approx 130 \text{ sec}^{-1}$, with spin exchange involving those methyl energy levels giving rise to the broad methyl resonance occurring ten times more frequently than with those methyl levels associated with the narrow resonance.

We can now estimate the time for spin diffusion to occur over a certain distance along the methylene chain, as well as the time for spin diffusion to occur between the terminal methyl group and its neighboring methylene protons on the same hydrocarbon chain. The time for spin diffusion in the latter case is just the reciprocal of the spin exchange rate, or $\approx 0.01 \text{ sec}$. For spin diffusion along the methylene chain, the successive spin exchanges along the various possible paths should be considered. Between methylene groups, spin exchange which occurs between protons on carbons separated by one methylene is much more efficient for effecting spin diffusion than the spin exchange between nearest neighbor inter-pair methylene protons, even though the spin exchange rates, W , are comparable for both processes. This is so because in the latter case the spin energy gets propagated a distance a along the hydrocarbon chain axis, whereas in the former case this distance is $2a$. The time for spin energy to diffuse over a distance d along the hydrocarbon chain is thus given by⁽⁷¹⁾

$$t \cong \frac{d^2}{W [a^2 + (2a)^2]}$$

This result predicts a time of ~ 0.15 sec for spin diffusion over 10 carbon-carbon bonds along the hydrocarbon chains of the lecithin molecules.

In the light of the above considerations, it is clear that the spin exchange rate between terminal methyl and methylene protons is much faster than the rate of spin-lattice relaxation ($1/T_1$) of a methyl group. This means that the terminal methyl protons are strongly coupled to the methylene chain protons, and must thereby share common heat sinks. Furthermore, because spin diffusion does occur over much of the methylene chain in a time shorter than the observed methylene T_1 , the bulk of the methylene chain protons do not serve as their own heat sinks in spin lattice relaxation. It is likely that the less mobile methylene groups near the glycerol backbone, and thus most distant from the actual heat sinks, have linewidths considerably greater than the average linewidths. Spin exchange among these protons would then be faster than the average rate for the chain methylenes, in which case the methylene chain would be sufficiently coupled that spin diffusion would occur over the entire chain in a time shorter than T_1 .

We point out, however, that it is not possible for the entire methylene chain to be relaxed solely via dissipation of the spin energy through the methyl heat sinks. This is because in general the measured T_1 of a strongly coupled spin system will be longer than the intrinsic T_1 of the relaxing spin by a factor of the ratio of the total number of spins coupled by spin diffusion to the number

of relaxing spins. ⁽⁷⁰⁾ Should relaxation of methylene protons be controlled by these methyl groups, the measured T_1 of ≈ 0.1 sec for the entire lecithin multilayer sample would imply an intrinsic T_1 of ≈ 0.01 sec for the methyl protons, a value which is \sim a factor of 3 shorter than the expected minimum possible methyl T_1 if the relaxation is purely of dipolar origin. Instead, the measured relaxation times indicate that the methyl group, together with perhaps 2-4 mobile methylene groups, serves as the heat sinks for the entire methylene chain.

7. Interpretation of T_1 data. The above considerations regarding spin diffusion in the lecithin multilayers suggest that the methylene chain protons are strongly coupled among themselves and are coupled to the lattice via some fraction of their number. In addition, it appears that the spin lattice relaxation behavior of the terminal methyl protons and the methylene protons of the hydrocarbon chains are interdependent. On the other hand, it could be said with some assurance that the choline methyl protons are not coupled to the protons on the hydrocarbon chains, although we expect that they are coupled to the two choline methylene groups. In the light of these considerations, interpretation of the data for the choline methyl groups can be made without qualification, since the T_1 measured for these protons is basically their intrinsic T_1 . However, since the terminal methyl protons are coupled to a very large spin system, namely the methylene protons, the precise

mechanism responsible for the terminal methyl T_1 is not clear. The T_1 observed for the bulk sample, however, can be considered as characteristic of the small number of the methylene protons which are acting as the heat sinks for the entire coupled spin system. The intrinsic value of T_1 for these methylene heat sinks would be considerably shorter than the observed bulk T_1 if these protons were not relaxing a large spin system.

We can now proceed to obtain a quantitative description of the motional state of the methyl and methylene groups of the lecithin molecule. We assume, for example, for a methylene pair, that the state of motion can be described in terms of a model in which the interproton magnetic dipolar vector reorients about the hydrocarbon chain axis with a correlation time τ_{\parallel} , and undergoes off-axis motion with a correlation time τ_{\perp} , with the off-axis motion restricted to excursions of at most $\Delta\beta$ from the average interproton vector reorientation $\bar{\beta}$.⁽³²⁾ Similarly, the motion of a methyl rotor can be described by two motional correlation times, τ_{\parallel} for the reorientation about the rotor axis, and τ_{\perp} for the off-axis excursions, as well as a range for the excursions of the rotor axis, $\Delta\theta'$. Using these motional models, we seek appropriate combinations of the parameters τ_{\parallel} , τ_{\perp} , $\Delta\beta$ or $\Delta\theta'$, which account for the following observations:

- (1) T_1 is a weak function of frequency, decreasing with decreasing frequency.
- (2) T_1 increases with increasing temperature at all

frequencies observed.

- (3) The magnetization recovery is exponential at all frequencies observed.

In our analysis we have modified the well known theory of Woessner⁽⁷²⁾ for relaxation of protons of methyl tops undergoing anisotropic reorientation to include the effects of motional restriction. The following expression has been obtained for an assembly of methyl rotors undergoing anisotropic and restricted motion:⁽³²⁾

$$\begin{aligned} \frac{1}{T_1} = & \frac{9}{4} \frac{\gamma^4 \hbar^4}{r^6} \left\{ \frac{1}{4} \frac{\overline{(\sin \theta' \cos \theta')^2}}{(\sin \theta' \cos \theta')^2} \cdot \frac{2 \tau_{\perp}}{1 + \omega_0^2 \tau_{\perp}^2} \right. \\ & + \frac{1}{8} \frac{\overline{\sin^2 \theta' (1 + \cos^2 \theta')}}{\sin^2 \theta' (1 + \cos^2 \theta')} \cdot \frac{2 \tau_c}{1 + \omega_0^2 \tau_c^2} \\ & + \frac{1}{4} \frac{\overline{(\sin^2 \theta')^2}}{(\sin^2 \theta')^2} \cdot \frac{2 \tau_{\perp}}{1 + 4 \omega_0^2 \tau_{\perp}^2} \\ & \left. + \frac{1}{8} \frac{\overline{(1 + 6 \cos^2 \theta' + \cos^4 \theta')}}{(1 + 6 \cos^2 \theta' + \cos^4 \theta')} \cdot \frac{2 \tau_c}{1 + 4 \omega_0^2 \tau_c^2} \right\} \end{aligned}$$

In this expression, $1/\tau_c = 1/\tau_{\perp} + 1/\tau_{\parallel}$, θ' is the orientation of the methyl rotor axis in the magnetic field, and the bars denote averaging over the appropriate range of $\Delta\theta'$. It should be noted that the intermolecular contribution to T_1 , neglected in the above expression, has been shown to be of the order of 20% of the

intramolecular relaxation rate for polymethylene chains. (73, 74)

An analogous expression can be derived to calculate the T_1 of methylene protons which are reorienting freely about an axis, \vec{c} . Here, θ' in the T_1 expression would denote the orientation of the \vec{c} axis in the magnetic field, and the angular functions would be averaged over the appropriate range of β ($\Delta\beta$). Because $\bar{\beta} = 90^\circ$ for methylene protons, this averaging over β is equivalent to similar averaging of the angular functions over excursions in θ' of the \vec{c} axis, and this latter procedure is actually used for convenience.

In order to clarify the above motional model, we now outline the method used to obtain the appropriate averages of the angular functions in the T_1 expression for the methyl protons. For a methyl rotor undergoing restricted motion, the rotor axis can wander over the angular range $\bar{\theta}' \pm \Delta\theta'$. This motion allows the rotor axis vector to trace out a cap on the surface of a unit sphere. For a given value of $\bar{\theta}'$, the angular averages in the T_1 expression may be obtained by averaging the angular functions over this range of angles. Statistical weighting of the angular functions must be included in the averaging procedure since the rotor axis has a greater probability of being at $\theta' = \bar{\theta}'$ than at any other angle, with $\theta' = \bar{\theta}' \pm \Delta\theta'$ being the least probable angles. Using the weighting function

$$\sin \left\{ (\pi/2) \left(\bar{\theta}' + \Delta\theta' - \theta' \right) / 2 \Delta\theta' \right\}$$

T_1 can thus be evaluated at any angle $\overline{\theta'}$ given $\Delta\theta'$, τ_{\parallel} , and τ_{\perp} . However, the samples contain methyl groups with all possible values of $\overline{\theta'}$. At any $\overline{\theta'}$ value, the number of methyl groups varies as $\sin \overline{\theta'}$. The T_1 which we determine experimentally is a composite of different T_1 values from protons with various average orientations of the axis vector relative to H_0 . Since some of these orientations are more probable than others, the magnetization recovery of the various parts of the sample is weighted by $\sin \overline{\theta'}$, and the sum of the magnetization recoveries is fitted to a single value of T_1 for comparison with experiment.

As anticipated, our calculations predict that only certain ranges of the variables τ_{\parallel} , τ_{\perp} and $\Delta\theta'$ ($\Delta\beta$) can account for the complex temperature and frequency dependence observed for the T_1 's. For the choline methyl protons, the observed T_1 and its temperature dependence (near room temperature) at 220 MHz and at 100 MHz was accounted for only with the following parameters:

$$\tau_{\parallel} = 1 \times 10^{-10} - 5 \times 10^{-11} \text{ sec}$$

$$\tau_{\perp} \geq 4 \times 10^{-7} \text{ sec}$$

$$\Delta\theta' \geq 60^\circ$$

Similarly, the measured T_1 values at 54 MHz, 22 MHz and 8.4 MHz, together with the observed temperature dependence (near room temperature), yielded:

$$\tau_{\parallel} = 1 \times 10^{-9} - 2 \times 10^{-10} \text{ sec}$$

$$\tau_{\perp} \geq 1 \times 10^{-7} \text{ sec}$$

$$\Delta\beta \geq 60^{\circ}$$

for the motional parameters of the methylene protons which are relaxing the coupled spin system. In these results, the restriction on $\Delta\theta'$ and $\Delta\beta$ arises from the calculated non-exponential magnetization recovery for $\Delta\theta'$, $\Delta\beta < 90^{\circ}$. In practice, the deviation from exponential behavior could be easily detected only for $\Delta\theta'$, $\Delta\beta \leq 60^{\circ}$. Since the experimental magnetization recovery plots were always exponential, we conclude that for our samples, $\Delta\theta \geq 60^{\circ}$.

The motional parameters for the terminal methyl group cannot be directly determined, because these methyl protons are coupled to the large methylene spin system, and are thereby affected in their relaxation behavior. Nonetheless, since the narrow methyl resonance is not strongly coupled to the methylene spin system, the intrinsic T_1 of the terminal methyl protons cannot be very different from the value of T_1 observed for the narrow methyl resonance. The motional parameters of our model may therefore be fitted to the observed T_1 data for the methyl resonance. The result of this treatment is that, for the terminal methyl protons on the hydrocarbon side chains, $\tau_{\parallel} = 1 \times 10^{-10} - 5 \times 10^{-11}$ sec and $\tau_{\perp} \geq 1 \times 10^{-7}$ sec.

8. Segmental motion of the hydrocarbon chain. The preceding analysis has permitted us to ascertain those molecular motions of the lecithin molecule which serve to couple the spin energy into the lattice. An earlier linewidth analysis has enabled us to comment on the degree of motional restriction. (32) The present T_1 studies confirm these linewidth results, but in addition permit the description of the molecular motion in the lecithin molecule in terms of certain motional correlation times. Such motional correlation times have a precise meaning in magnetic resonance theory.

In a system as complex as a lecithin multilayer, interpretation of the correlation times τ_{\parallel} and τ_{\perp} may present some difficulty. However, in one of our earlier papers evidence was presented to suggest that only motions which preserve the overall orientation of the chain perpendicular to the multilayer surface are allowed. In fact, the off-axis motion, corresponding to τ_{\perp} , has been ascribed to kink formation in lecithin multilayers (32, 75) (or "crankshaft motion", as kinks have been called in polymers). (76) Kink formation results from $^+$ gauche rotation about one carbon-carbon single bond, simultaneous with $^-$ gauche rotation about another carbon-carbon bond which is separated from the first by one or more bonds. The intra-pair, inter-proton vector on methylene groups undergoing such rotation is taken through an angle of approximately 60° by this motion. Kink formation is expected to be most rapid near the free end of the methylene chain, since

the initial activation energy is lowest there. ⁽⁷⁵⁾ On the other hand, because of steric restrictions, the end of the methylene chain which is bonded to the glycerol backbone undergoes less rapid kink formation. On this basis, the off-axis motion of the methylene groups would be increasingly more rapid toward the methyl end of the chain.

The other type of methylene motion, described by τ_{\parallel} , is reorientation around the chain axis. The way in which such a reorientation comes about is of interest. The molecule as a whole cannot be reorienting at this rate of $\approx 10^9 \text{ sec}^{-1}$, as indicated by the rate of $\approx 10^6 \text{ sec}^{-1}$ for comparable single chain molecules, ⁽⁷⁷⁾ which have a much smaller moment of inertia than does the double chain lecithin, and also whose cylindrical symmetry permits reorientation without great steric restraints, again different from lecithin. One type of motion which is occurring rapidly, and which could result in reorientation about the chain axis, is torsional oscillation about carbon-carbon single bonds. The motion about one bond is of low amplitude ($< 20^\circ$) and very fast, $\approx 10^{14} \text{ sec}^{-1}$. ⁽⁷⁸⁾ This frequency is much too high to be an effective source of T_1 relaxation. However, a long series of such torsional oscillators, weakly coupled, would give rise to larger amplitude motions of lower frequency, simply from statistical fluctuations in the phase of the many oscillations.

A quantitative treatment of the problem of a large number (e. g. 16) of weakly coupled torsional oscillators which are loosely

confined to a cylinder would be exceedingly difficult. We do not attempt even an approximate solution of such a problem. We only point out that such oscillations will give rise to a distribution of correlation times for motion around the methylene chain axis. These motions are bounded at the high frequency, low amplitude end by the single bond oscillation frequency of $\approx 10^{-14}$ sec. An example of a higher amplitude, lower frequency motion occurs when all oscillators are rotating in the same direction. The frequency of this occurrence is approximately $(\frac{1}{2})^{16} \times 10^{14} \approx 1 \times 10^9$ (for a chain of 16 methylene groups). Our experimentally derived result that $\tau_{\parallel} = 1 \times 10^{-9} - 2 \times 10^{-10}$ probably represents a weighted mean for a distribution of motions of the methylene group heat sinks.

VI. Conclusions

This investigation clearly shows the importance of choosing experimental techniques which are appropriate for studying the nmr behavior of the complex aqueous lecithin bilayer system. Instruments such as pulse or wide-line nmr spectrometers must be used in order to observe the entirety of the broad nmr signal. In addition, much narrower nmr signals are present which cannot be resolved using such equipment designed for the study of solids. For this reason, the Delayed Fourier Transform technique was utilized to isolate the narrow methyl resonances from the bulk of

the signal. These resonances are thereby sufficiently distinct from each other and from the bulk of the signal to enable us to determine the T_1 values and the intensities of the individual methyl resonances.

The linewidth of the pmr spectrum of aqueous lecithin bilayers is not a suitable measurement of the spin-spin relaxation time because of the disproportionate weight given to the narrower resonances. These chemically shifted narrow methyl resonances also introduce a significant field dependence of the linewidth which can lead to the incorrect inference that magnetic dipolar interactions are not the dominant line broadening mechanism. For a complex spin system such as lecithin bilayers, the value of T_2 determined from the free induction decay is a reliable measure of the spin-spin relaxation and does provide insight into the relaxation mechanism.

NMR is a particularly useful technique for examining molecular motion. In contrast to other methods such as electron spin resonance or fluorescence which require a bulky probe molecule, nmr uses only the nuclear spins as labels. Because the lecithin molecule contains chemically shifted spins, the lecithin is effectively labelled at both the polar head group and at the hydrophobic core of the bilayer. As an example of the use of these natural labels, Hsu and Chan have exploited the specific line broadening of the choline methyl resonance by valinomycin to show that this antibiotic interacts with the bilayer predominantly

at the polar head group. (67)

This paper also demonstrates how the motional mechanisms responsible for the spin lattice relaxation times of the lecithin methyl and methylene protons can be determined from a study of the temperature and magnetic field dependence of the spin-lattice relaxation rate. For choline and terminal methyl protons, the motion which is most effective for T_1 relaxation was shown to be rapid reorientation around the methyl rotor axis, with a smaller influence from the slower, off-axis motion. The hydrocarbon chain methylene protons are most likely relaxed primarily via torsional oscillations of the methylene chain, with a smaller influence on the relaxation rate from kink formation. Spin diffusion was shown to have a pronounced influence on the T_1 of the hydrocarbon chain methylene protons. Furthermore, spin diffusion was demonstrated to give rise to mutual interdependence of the spin-lattice relaxation behavior of the terminal methyl and chain methylene protons. This study of spin-lattice relaxation behavior in lecithin multilayers complements and augments a recent lecithin linewidth study from this laboratory. (32) In our earlier work, the nmr lineshape was shown to be a sensitive monitor of the details of slow molecular motions. This present work indicates that the spin-lattice relaxation is sensitive primarily to the time scale of the more rapid molecular motions.

References

1. G. F. Azzone, E. Rossi and A. Scarpa, "Regulatory Functions of Biological Membranes," J. Jarnefelt, ed., Elsevier Publishing Co., Amsterdam (1968).
2. E. D. Korn, Science, 153, 1491 (1966).
3. F. Haurowitz, "Chemistry and Biology of Proteins," Chapter 9, Academic Press, Inc., New York (1950).
4. L. L. M. Van Deenen, "Regulatory Functions of Biological Membranes," J. Jarnefelt, ed., Elsevier Publishing Co., Amsterdam (1968).
5. W. Pigman, "The Carbohydrates," Chapter 12, Academic Press, Inc., New York (1957).
6. J. W. McBain, "Colloid Chemistry," J. Anderson, ed., Chapter 1, Chemical Catalog Co., Inc., New York (1926).
7. M. de Broglie and E. Friedel, Comptes Rend., 176, 738 (1923).
8. J. W. McBain and M. C. Field, J. Phys. Chem., 30, 1545 (1926).
9. J. W. McBain and G. M. Langdon, J. Chem. Soc. London, 127, 852 (1925).
10. D. M. Small, J. Amer. Oil Chem. Soc., 45, 108 (1968).
11. E. Gorter and F. Grendel, J. Exptl. Med., 41, 439 (1925).
12. H. A. Davson and J. F. Danielli, J. Cell. Comp. Physiol., 5, 495 (1935).
13. F. O. Schmitt, R. S. Bear and K. J. Palmer, J. Cell. Comp. Physiol., 18, 31 (1941).

14. J. D. Robertson, Symp. Biochem. Soc., 16, 3 (1959).
15. E. D. Korn, J. Gen. Physiol., 52, 257 (1968).
16. C. W. F. McClare, Nature, 216, 766 (1967).
17. M. Glaser, H. Simpkins, S. J. Singer, M. Sheetz and S. I. Chan, Proc. Nat. Acad. Sci., 65, 721 (1970).
18. M. P. Sheetz and S. I. Chan, Biochemistry, 11, 548 (1972).
19. J. M. Steim, M. E. Tourtellote, J. C. Reinert, R. N. McElhaney and R. L. Rader, Proc. Nat. Acad. Sci., 63, 104 (1969).
20. J. F. Blazykt and J. M. Steim, Biochim. Biophys. Acta, 266, 737 (1972).
21. D. M. Engelman, J. Mol. Biol., 47, 115 (1970).
22. Y. K. Levine and M. H. F. Wilkins, Nature, New Biol., 230, 69 (1971).
23. M. H. F. Wilkins, A. E. Blaurock and D. M. Engelman, Nature, New Biol., 230, 72 (1971).
24. W. L. Hubbell and H. M. McConnell, Proc. Nat. Acad. Sci., 63, 16 (1969).
25. S. A. Henry and A. D. Keith, Chem. Phys. Lipids, 7, 245 (1971).
26. D. Papahadjopoulos and J. C. Watkins, Biochim. Biophys. Acta, 135, 639 (1967).
27. D. M. Michaelson, A. F. Horwitz and M. P. Klein, Biochemistry, 12, 2637 (1973).
28. K. M. Keough, E. Oldfield, D. Chapman and P. Bergnon, Chem. Phys. Lipids, 10, 37 (1973).

29. H. T. Tien and A. L. Diana, Chem. Phys. Lipids, 2, 55 (1968).
30. D. Papahadjopoulos and L. Weiss, Biochim. Biophys. Acta, 183, 417 (1969).
31. H. Hauser, M. C. Phillips and M. Stubbs, Nature, 239, 342 (1972).
32. C. H. A. Seiter and S. I. Chan, J. Amer. Chem. Soc., in press.
33. M. P. Sheetz and S. I. Chan, Biochemistry, 11, 4573 (1972).
34. S. I. Chan, G. W. Feigenson and C. H. A. Seiter, Nature, 231, 110 (1971).
35. J. Charvolin and P. Rigny, J. Magn. Resonance, 4, 40 (1971).
36. G. J. T. Tiddy, Nature, 230, 136 (1971).
37. J. J. DeVries and H. J. C. Berendsen, Nature, 221, 1139 (1969).
38. K. D. Lawson and T. J. Flautt, Mol. Cryst., 1, 241 (1966).
39. Z. Veksli, N. J. Salsbury and D. Chapman, Biochim. Biophys. Acta, 183, 434 (1969).
40. E. G. Finer, A. G. Flook and H. Hauser, Biochim. Biophys. Acta, 260, 59 (1972).
41. S. A. Penkett, A. G. Flook and D. Chapman, Chem. Phys. Lipids, 2, 273 (1968).
42. E. R. Andrew and R. Bersohn, J. Chem. Phys., 18, 159 (1950).
43. W. L. Hubbell and H. M. McConnell, Proc. Nat. Acad. Sci., 61, 12 (1968).
44. E. J. Shimshick and H. M. McConnell, Biochemistry, 12, 2351 (1973).
45. W. L. Hubbell and H. M. McConnell, Proc. Nat. Acad. Sci.,

- 64, 20 (1969).
46. J. Seelig, J. Amer. Chem. Soc., 92, 3881 (1970).
 47. V. Luzzati, "Biological Membranes," D. Chapman, ed., Academic Press, Inc., New York (1968).
 48. V. Luzzati, T. Gulik-Krzywicki and A. Tardieu, Nature, 218, 1031 (1968).
 49. F. Reiss-Husson, J. Mol. Biol., 25, 363 (1967).
 50. D. M. Small, J. Lipid Res., 8, 551 (1967).
 51. R. P. Rand and V. Luzzati, Biophys. J., 8, 125 (1968).
 52. A. E. Blaurock and M. H. F. Wilkins, Nature, 223, 906 (1969).
 53. E. Sackman and H. Träuble, J. Amer. Chem. Soc., 94, 4482 (1972).
 54. M. B. Feinstein, L. Spero and H. Felsenfield, FEBS Letters, 6, 245 (1970).
 55. R. B. Freedman and G. K. Radda, FEBS Letters, 3, 150 (1969).
 56. J. Vandekooi and A. Martonosi, Arch. Biochem. Biophys., 133, 153 (1969).
 57. B. D. Ladbrooke and D. Chapman, Chem. Phys. Lipids, 3, 304 (1969).
 58. H. -J. Hinz and J. M. Sturtevant, J. Biol. Chem., 247, 6071 (1972).
 59. N. J. Salsbury, A. Darke and D. Chapman, Chem. Phys. Lipids, 8, 142 (1972).
 60. S. Kaufman, J. M. Steim and J. H. Gibbs, Nature, 225, 743 (1970).

61. J. R. Hansen and K. D. Lawson, Nature, 225, 542 (1970).
62. D. Papahadjopoulos, K. Jacobson, S. Nir and T. Isac, Biochim. Biophys. Acta, 311, 330 (1973).
63. K. van Putte and G. J. N. Egmond, J. Magn. Resonance, 4, 236 (1971).
64. J. T. Daycock, A. Darke and D. Chapman, Chem. Phys. Lipids, 6, 205 (1971).
65. W. S. Singleton, M. S. Gray, M. L. Brown and J. L. White, J. Amer. Oil Chem. Soc., 42, 53 (1965).
66. C.H. A. Seiter, G. W. Feigenson, S. I. Chan and M.-C. Hsu, J. Amer. Chem. Soc., 94, 2535 (1972).
67. M.-C. Hsu and S. I. Chan, Biochemistry, 12, 3872 (1973).
68. N. J. Salsbury, D. Chapman and G. P. Jones, T. Farad. Soc., 65, 1554 (1969).
69. N. Bloembergen, Physica, 15, 386 (1949).
70. J. E. Anderson and W. P. Slichter, J. Phys. Chem., 69, 3099 (1965).
71. A. Abragam, "The Principles of Nuclear Magnetism," Chapter 5, Oxford University Press, London (1961).
72. D. E. Woessner, J. Chem. Phys., 36, 1 (1962).
73. A. G. Lee, N. J. M. Birdsall and J. C. Metcalfe, Biochemistry, 12, 1650 (1973).
74. T. L. Pendred, A. M. Pritchard and R. E. Richards, J. Chem. Soc. (A), 1009 (1966).
75. H. Trauble, J. Memb. Biol., 4, 193 (1971).

76. R. F. Boyer, J. Polymer Sci. C, 14, 3 (1966).
77. R. F. Grant and B. A. Dunnell, Can. J. Chem., 38, 2395 (1960).
78. P. J. Flory, "Statistical Mechanics of Chain Molecules," Inter-science, New York (1969).

PROPOSITION I

The potential usefulness of the Waugh multiple-pulse technique for resolving the chemical shifts of dipolar-broadened nmr lines has not yet been realized. In part, this is because the degree of motion characteristic of many molecules of interest may be enough to destroy the averaging effects of the Waugh pulse sequence, although the motion may not be sufficient to give sharp nmr lines. Thus, the least mobile molecules are the best subjects for the Waugh sequence. It is proposed to use the Waugh multiple-pulse technique to narrow the nmr signals from large enzymes in solution and from membrane-bound enzymes, in order to identify the chemical groups of the active center of the enzyme.

Until a very few years ago, the study of solids by nmr relied exclusively on the application of the nmr relaxation methods, i. e., studies of T_2 , T_1 and $T_{1\rho}$. The information contained in the chemical shifts could not be obtained, because these shifts are so much smaller than the dipolar line-broadening interaction in solids. As an example, for the protons in solid lecithin in a magnetic field of 23.5 kgauss, the chemical shifts, which range over 800 Hz, are completely obscured by the dipolar linewidth, which is $\sim 20,000$ Hz. (1)

In the late 1960's, J. S. Waugh, (2) by developing a method discovered by E. R. Andrew, (3) succeeded in removing approximately 99% of the dipolar interaction in solid CaF_2 and $\text{CaSO}_4 \cdot 4\text{H}_2\text{O}$, enabling

the chemical shifts of these substances to be observed for the first time. Recent refinements of the Waugh technique have led to $\sim 99.9\%$ effective removal of the dipolar interaction. ⁽⁴⁾ This means that now even the relatively small proton chemical shifts of solids, and of course the larger ^{13}C , ^{19}F and ^{31}P chemical shifts can be measured and exploited.

The mechanism by which the Waugh multiple-pulse sequence averages the dipolar interaction can be understood by referring to the dipolar Hamiltonian, ⁽²⁾

$$\mathcal{H}_d = \gamma^2 \hbar \sum_{i < j} \sum r_{ij}^{-5} (\vec{r}_{ij} \cdot \vec{r}_{ij} - 3 z_{ij} z_{ij}) (\vec{I}_i \cdot \vec{I}_j - 3 I_{zi} I_{zj})$$

where γ = magnetogyric ratio

\hbar = Planck's constant

\vec{r}_{ij} = vector joining spins i and j

\vec{I} = spin vector

Either term in parenthesis on the right hand side of the above equation can be replaced by its representation in polar coordinates ($3 \cos^2 \theta - 1$). It can be shown that if all the \vec{r}_{ij} vectors are rotated uniformly about an axis at $\theta = 54^\circ 44'$ to the external magnetic field, and if this averaging takes place in a time less than T_2 , then the dipolar interaction falls to zero. ⁽²⁾ This experiment, the physical rotation of a solid sample about an axis inclined at $54^\circ 44'$ to the external magnetic field direction, has been successfully performed by Andrew et al. to resolve ^{31}P chemical shifts in solid P_2Cl_{10} . ⁽³⁾

An equivalent averaging procedure can be performed on the spin coordinates, \vec{I} , rather than the space coordinates, \vec{r} . This experiment, first performed by Waugh,⁽²⁾ consists of a series of intense radiofrequency pulses applied to the sample which rotate the spin vector about appropriate axes. The advantage of the Waugh pulse sequence over sample spinning at $54^\circ 44'$ is that the pulse sequence can be applied much faster than the sample can be spun, permitting this averaging to be performed on samples with T_2 as short as $10 \mu\text{sec}$.

The problem with the application of this technique to any large molecule which gives broad nmr lines which we would like to narrow is that any molecular motion during the course of the pulse sequence will randomly modulate the spatial term in the dipolar Hamiltonian, thereby destroying the orderly averaging done on the spin term. To be more precise, if the total time for a complete cycle of the Waugh sequence is 5×10^{-6} sec, then any motion which significantly modulates the dipolar interaction at a rate faster than 10^6 sec^{-1} will eliminate the dipolar averaging effect.

In order to determine which systems may be profitably examined with the Waugh technique, we now describe in general terms the kinds of motion characteristic of large molecules. One sort of motion is overall tumbling of the molecule in solution. For molecules with m. w. $\approx 10^4$, nmr lines will be sharp, simply from the averaging of the dipolar interaction by rapid tumbling. Local, or segmental motion also contributes to line-narrowing. Thus, for

any molecule in solution of m. w. $\approx 10^4$, and even for larger molecules which possess sufficient segmental motion, nmr lines are sharp and the Waugh technique is not useful or necessary. For molecules of m. w. $< 10^6$ in solution, overall tumbling, and therefore modulation of the dipolar interaction, is fast enough to destroy the dipolar averaging effects of the Waugh pulse sequence. And whatever the molecular size, if there is sufficient local motion, the Waugh technique will not be useful.

Thus, the biological domain of the Waugh technique is restricted to molecules of m. w. $> 10^6$, and to bound, e. g. membrane bound molecules. Even in these cases, segmental motion must be either severely restricted (that is, bounded) or else slower than 10^6 sec^{-1} .

The systems of choice, from the above motional considerations, as well as from consideration of the importance of such studies, are large enzymes in solution, and membrane-bound enzymes. The significance of enzyme studies will not be dealt with here. However, we note the difficulty of studying the molecular details of large enzymes and membrane-bound enzymes. In such systems, the usual spectroscopic techniques are plagued with broad and overlapping signals from the various amino acids. ⁽⁵⁾ Chemical methods such as amino acid modification or selective peptide cleavage require almost prohibitively great systematic labor to obtain information about very large molecules. ⁽⁶⁾

Two classes of experiments utilizing the Waugh pulse

sequence will now be proposed. In the first, the overall and the segmental immobility of certain enzymes will enable the Waugh technique to produce an nmr spectrum containing many sharp lines. Perhaps a suitable system would be the multi-enzyme complex of pig heart pyruvate dehydrogenase (m. w. $\sim 7.4 \times 10^6$)⁽⁷⁾ or the membrane-bound enzyme, glucose-6-phosphatase.⁽⁸⁾ There is an element of doubt as to the suitability of these molecules, because the extent of segmental molecular motion is not known. The presumably sharp resonances in these nmr spectra could then be assigned by the usual nmr techniques of chemical shift measurement, spin decoupling and isotopic substitution. Furthermore, the active center of the enzymes may prove to be particularly easy to assign: chemical exchange of the substrate will selectively broaden the sharp peaks from the active center, if the chemical shifts and the exchange rate are of the appropriate magnitude.

A second class of Waugh pulse experiments would be performed on large or bound enzymes which did possess significant segmental motion. In this case, the enzyme will have a broad-line spectrum after the Waugh pulse sequence. However, upon binding to a substrate, if the enzyme-substrate complex is sufficiently long-lived, the spins whose motion is slowed down or restricted will now appear as sharp lines after the Waugh pulse sequence. These sharp peaks are expected to be just those of the part of the enzyme which binds the substrate. The assignment of these relatively few sharp peaks against the background of resonances still

broad because of local molecular motion might be relatively easy. An enzyme which might be amenable to this technique is the membrane-bound ATP phosphohydrolase (ATPase).⁽⁹⁾ This enzyme is found throughout an organism, but especially in muscle, where mechanical work is performed, and in membranes where energy release is coupled to ion pump operation. ATPase forms a stable complex with the inorganic phosphate reaction product above 25°C. It also forms a stable complex with ATP in acidic media in the presence of excess ATP.

It should be emphasized that the choice of any particular enzyme system may prove to be inappropriate, because the extent of local motion is not known in advance. However, an enzyme should certainly be chosen which has very slow overall tumbling, i. e., a large or membrane-bound enzyme. For such enzymes, the Waugh pulse sequence may prove to be a particularly simple way to identify and characterize the substrate-specific binding site.

References

1. G. W. Feigenson, Ph.D. thesis (1973).
2. U. Haeberlen and J. S. Waugh, Phys. Rev., 185, 185 (1969).
3. E. R. Andrew, A. Bradbury, R. G. Eades and G. J. Jenks, Nature, 188, 1096 (1960).
4. R. W. Vaughan, D. D. Elleman, L. M. Stacey, W.-K. Rhim and J. W. Lee, Rev. Sci. Instr., 43, 1356 (1972).
5. S. N. Timasheff, "The Enzymes," volume 2, P. D. Boyer, ed., Academic Press, Inc., New York (1970).
6. B. L. Vallee and J. F. Riordan, Ann. Rev. Biochem., 38, 733 (1969).
7. L. J. Reed and D. J. Cox, "The Enzymes," volume 1, P. D. Boyer, ed., Academic Press, Inc., New York (1970).
8. J. L. E. Ericsson, J. Histochem. Cytochem., 14, 366 (1966).
9. H. Bader, R. L. Post and D. H. Jean, Biochim. Biophys. Acta, 143, 229 (1967).

PROPOSITION II

Considerable evidence exists that an important part of the immune response depends in some way upon the "cooperation" between thymus-derived cells (T-cells) and bone marrow-derived cells (B-cells).⁽¹⁻³⁾ An experiment is proposed to test one hypothesis which has been advanced to explain the cooperation between T-cells and B-cells.

The immune response to low-level antigenic stimulation requires the presence of normal T-cells. This requirement was demonstrated by Isokovic et al., who showed that thymus grafts from normal mice restore responsiveness to thymectomized mice, whereas such grafts from tolerant mice do not.⁽⁴⁾ Furthermore, Mitchell and Miller showed that the T-cells do not secrete antibody, but that B-cells do.⁽⁵⁾

Several hypotheses have been advanced to explain the role of T-cells in the immune response.^(6, 7) All such hypotheses propose that the B-cells are stimulated in some way by the T-cells. The three proposed mechanisms of stimulation are as follows:

(1) The T-cells provide non-specific nutrient materials, such as nucleotides or nucleotide precursors, which enable the B-cells to multiply. A variant of this idea is that a non-specific pharmacologically active agent is released by stimulated T-cells, which in turn induces B-cells to be immunologically active.

(2) There is transfer of specific information from antigen

stimulated T-cells to B-cells. After this event, the B-cells produce the appropriate antibodies.

(3) The T-cells accumulate antigen on their surface. This localized high concentration of antigen is seized by the B-cells, which then are stimulated to produce antibody and to multiply.

The requirement for testing either of the first two hypotheses is a method capable of distinguishing small amounts of ordinary cellular material from one cell, the T-cell, which has been transferred to another cell, the B-cell. The last hypothesis, however, would be much easier to test, because extra-cellular material is involved, which can readily be labelled.

The labelling method proposed here is an immunofluorescence method. The advantages of immunofluorescence labels are sensitivity of detection of small quantities of label, and specificity of the label for particular molecules.⁽⁸⁾ Immunofluorescent labels have been attached to both antibodies and to antigens.⁽⁹⁾

An outline of an experiment designed to test hypothesis (3), that T-cells accumulate antigen and thereby stimulate B-cells, is given below:

1. Diphtheria toxoid is labelled with the green fluorescent dye, fluorescein (label 1).
2. Rabbit (anti-mouse immunoglobulin) antibody is labelled with the orange-red fluorescent dye, rhodamine sulphonyl chloride (label 2).
3. Mice are immunized with label 1.

4. The thymus from the immunized mice is grafted into previously thymectomized mice.

5. Lymphocytes from the previously thymectomized but now thymus-grafted mice are removed, and incubated in tissue culture agar.

6. The cells in tissue culture are washed with label 2, and rinsed.

7. In a fluorescence microscope, some cells, and their immediate surroundings, will show up orange-red, because of antibody produced binding to label 2.

8. All cells which are orange-red, i. e., identified as antibody producers, are examined for additional faint green fluorescence. The presence of green fluorescence would show that antigen which was originally coating T-cells had actually migrated to B-cells, thereby stimulating antibody production.

The detection of green fluorescence in tissue-cultured B-cells would then support the hypothesis of Mitchison that the T-cells act by concentrating antigen on their surface, and in turn stimulating B-cells to produce antibody. However, it is possible that this method, which relies upon detection of only a small amount of fluorescent label on a cell surface, might not be sufficiently sensitive. Part of this sensitivity problem could be obviated by using an antigen, e. g. diphtheria toxoid, which is extremely heavily labelled with fluorescein.

The role of the macrophage in the immune response has also been ascribed to their ability to concentrate antigen, and to thereby

stimulate antibody production by B-cells. ⁽⁶⁾ This role for the macrophage could be tested in a manner similar to the test proposed above for the role of T-cells. In the case of the macrophage, thymectomy would not be necessary, but instead simply a transfer of macrophages from animals which had been immunized with fluorescent dye labelled antigen, to un-immunized animals. The B-cells from the latter would then be tested as above for both antibody production and the presence of the labelled antigen.

References

1. H. N. Claman and E. A. Chaperon, Transplant Rev., 1, 92 (1969).
2. J. F. A. P. Miller and G. F. Mitchell, Transplant Rev., 1, 3 (1969).
3. R. B. Taylor, Transplant Rev., 1, 114 (1969).
4. K. Isakovic, S. B. Smith and B. H. Waksman, J. Exptl. Med., 122, 1103 (1965).
5. G. F. Mitchell and J. F. A. P. Miller, J. Exptl. Med., 128, 821 (1968).
6. N. A. Mitchison in "Immunological Tolerance," M. Landy and W. Braun, eds., pp. 115-124, Academic Press, Inc., New York (1969).
7. J. F. A. P. Miller in "Immunological Tolerance," M. Landy and W. Braun, eds., p. 133, Academic Press, Inc., New York (1969).
8. A. H. Coons, Ann. N. Y. Acad. Sci., 177, 5 (1971).
9. R. G. White, Nature, 182, 1383 (1958).

PROPOSITION III

It is proposed to use thermal analysis to investigate the properties of mixed lipid systems.

The phospholipid bilayer is thought to be the structural basis of biological membranes. This structural role arises from the natural formation of the two dimensional bilayer from phospholipids and water. This strictly structural aspect of the phospholipids gives no hint as to the role of the individuality of the lipids.

Since the basic bilayer structure of membranes is adequately explained without recourse to the different characteristics of the various lipids, it is possible that the differences among the lipids are associated in some way with the functioning of the membrane. If the functional aspects of a biomembrane are assigned primarily to the proteins, e. g. solute transport, chemical reactions at an interface, then perhaps one basis of lipid diversity is selective interaction of lipids with the chemically diverse proteins, i. e. specific lipids are required for the activity of specific proteins. Support for this idea of lipid specificity for proteins comes from studies which show a dependency of enzyme activity on lipid composition. (1-3)

Another possible role for phospholipids is that they take a more direct part in membrane function. A possible reflection of this would be the segregation of lipids in the bilayer into discrete liquid crystal patches of each lipid type. If such segregation is not spontaneous, it could perhaps be induced by the presence, for example,

of certain proteins or salts. Such patches would have distinctive surface properties, e. g. an array of zwitterions from phosphatidyl choline as compared to an array of negative charges from phosphatidyl serine at high pH. These arrays, possessing a degree of order characteristic of the liquid crystal phase, could exhibit cooperative effects in response to local events. For example, the adsorption of Ca^{++} by a patch of negatively charged phosphatidyl serine might induce a structural rearrangement of the lipid molecules which would allow Cl^- to penetrate the bilayer. Conversely, the Ca^{++} might cause a pronounced rigidity of the patch of lipid, thus making the patch relatively impermeable. NMR studies by Hsu and Chan appear to indicate that cooperative effects occur in the bilayer surface in response to small amounts of adsorbed valinomycin.⁽⁴⁾ In summary, the existence of discrete patches of lipids could have biological implications which would not be associated with a homogeneous liquid crystal mixture of phospholipids.

A method of potentially great usefulness in the study of lipid mixtures is thermal analysis. Either differential scanning calorimetry (DSC) or differential thermal analysis (DTA) could be used. The difference between these methods is that in DSC a measured quantity of heat per unit time is delivered to the sample, thereby enabling the simple determination of the thermodynamic quantities ΔH and ΔS for a phase transition, whereas in DTA the sample and a reference are heated at the same rate and their temperature difference is recorded. Although the thermodynamic quantities are not

simply determined by using DTA, either this method or DSC would be suitable for the study proposed here, which only involves the construction of phase diagrams.

This proposed research involves the evaluation of the selectivity of proteins for the various lipids, and the search for the existence of two-phase liquid crystal regions, i. e., segregated lipid patches. Both of these studies can be pursued by constructing and examining (binary) temperature-composition phase diagrams, using thermal analysis.

With binary mixed lipid systems, the phase behavior documented to date may be described as mutual solubility in the liquid crystal phase, with limited or complete mutual solubility in the crystal phase.^(5, 6) The presence of an additive could affect the mixed lipid system in one of three ways, assuming insolubility of the additive in the crystal phase: (1) the additive is non-interacting and has no effect, (2) the additive is approximately equally soluble in either lipid, and thereby increases the mutual solubility of the lipids, (3) the additive selectively interacts with one of the lipids, thereby decreasing the mutual solubility of the lipids.⁽⁷⁾ Effect (2) would lead to an observed increase in the extent of the one-phase region of the phase diagram, whereas effect (3) would lead to an increase in the extent of the two-phase region.

In general, we expect a protein which interacts primarily with the lipid head group region to show the latter behavior, since the head groups differentiate the phospholipid classes. A protein

which interacts with the hydrocarbon region of the lipids would be much less selective of lipid classes, and would probably increase mutual solubility of the lipids.

The search for lipid combinations, perhaps in the presence of an additive, which would give rise to a two-phase liquid crystal region is straightforward: a horizontal line in the binary phase diagram, above which only the liquid crystal is present, is the boundary of such a two-phase liquid crystal region.⁽⁸⁾ In the thermal analysis measurements, samples of the composition range spanned by this line all melt sharply at precisely the same temperature. This line also has the interesting property of representing a continuous series of "triple-points", i. e., three phases in equilibrium.

References

1. G. S. Levey, J. Biol. Chem., 246, 7405 (1965).
2. J. Seelig, Eur. J. Biochem., 21, 17 (1971).
3. R. D. Mavis and P. R. Vagelos, J. Biol. Chem., 274, 652 (1972).
4. M. -C. Hsu and S. I. Chan, Biochemistry, 12, 3872 (1973).
5. B. D. Ladbrooke and D. Chapman, Chem. Phys. Lipids, 3, 304 (1969).
6. E. J. Shimshick and H. M. McConnell, Biochemistry, 12, 2351 (1973).
7. A. Findlay and W. Thomas, "International Critical Tables," volume 4, E. W. Washburn, ed., McGraw-Hill Book Co., New York (1928).
8. J. E. Ricci, "The Phase Rule," Chapter 8, D. Van Nostrand Co., Inc., Toronto (1951).

PROPOSITION IV

The mechanisms of ion transport through biological membranes are of considerable interest. In general, model membranes such as lipid bilayers, sonicated lipid vesicles, and black lipid films are used instead of real biological membranes. The problems of isolation and characterization of real biological carrier or "permease" molecules are circumvented by using model permeability enhancers termed ionophores. It is proposed here to study a model of an alkali cation, Tl^+ , by nuclear magnetic resonance, in the presence of model biological membranes and model permeability enhancers.

The nuclear magnetic resonance (nmr) study of potassium ion transport has been limited to the proton magnetic resonance (pmr) study of ionophores and K^+ -ionophore complexes, because the sensitivity of nmr for K^+ is so low. The Tl^+ ion has the same charge and approximately the same ionic radius as the K^+ ion. Furthermore, the sensitivity of nmr is 2000 times greater for Tl^+ than for K^+ . Thus, Tl^+ is the ion of choice as a model for K^+ .

The kinetics of complexation of Tl^+ with a number of ionophores would be studied in organic solvents. The advantage of preliminary studies in organic solvents is that the medium is homogeneous, thus avoiding surface effects. Ionophores such as valinomycin and monensin, which are believed to act as ion carriers, ⁽¹⁾ would be compared with the alleged pore-formers,

gramicidin S and nystatin. ⁽²⁾ The stoichiometry of such complexes is of particular interest, because the carriers are expected to form stoichiometric, probably 1:1 complexes, whereas the pore-formers might exhibit multi-molecular complexes, or perhaps no stoichiometric complexes at all. The exchange rate could be fast, slow, or intermediate, and is expected to depend on both the nature of the solvent and the ionophore. For example, K^+ -valinomycin exchange is slow in chloroform, ⁽³⁾ whereas K^+ -nonactin exchange is rapid in acetone. ⁽⁴⁾ The values of the exchange rate and the binding constant can be determined from the linewidths and chemical shifts of the Tl^+ resonance. ⁽⁵⁾

The more complex system of Tl^+ , ionophore, and aqueous lipid bilayer is expected to provide more insight into actual ion transport. The presence of the bilayer-water interface may be important, and the effect of the bilayer on the Tl^+ -ionophore exchange rate and binding constant would be determined by Tl^+ nmr. If it happens that sufficient Tl^+ actually enters the bilayer interior to give a detectable nmr signal, then the nature of the Tl^+ -ionophore complex would be of great interest, since it is expected that carrier and pore-forming ionophores complex ions quite differently within the membrane. It may then be possible by Tl^+ nmr to distinguish various transport mechanisms. For example, pore formation would not involve a 1:1 complex between ionophore and ion, whereas a free carrier mechanism would involve such a complex. Another transport mechanism, the so-called "carrier relay" mechanism,

postulates exchange of the ion between ionophore molecules within the membrane. ⁽⁶⁾ This proposed mechanism would involve Tl^+ chemical shifts and exchange rates which could in principle be determined by Tl^+ nmr.

In all of these bilayer- Tl^+ -ionophore studies, the nature of the lipid and the ionophore could be varied. In particular, a system would be sought which provided a sufficient concentration of Tl^+ within the bilayer to produce a detectable nmr signal. If a strong nmr signal could be observed, then the value of the Tl^+ correlation time could be determined. This could be conveniently done by measuring the Tl^+ spin-lattice relaxation time (T_1) as a function of the external magnetic field strength. Because the value of T_1 is at a minimum when the correlation time is approximately equal to the inverse of the Larmor precession frequency, a plot of T_1 vs. magnetic field strength will change abruptly when this equality obtains, and will then become invariant, if there are no other distinct motional states of the Tl^+ . However, if there exist more than one motional state for the Tl^+ , for example, Tl^+ free in the bulk water, Tl^+ -ionophore complex on the bilayer surface, and Tl^+ -ionophore complex within the bilayer interior, then each of these motional states could be detected as an abrupt change in the variation of T_1 with magnetic field strength, with the different motional states corresponding to characteristic values of the inverse Larmor precession frequency.

In summary, Tl^+ nmr could be used to determine exchange

rates, binding constants, and motional correlation times for Tl^+ -ionophore complexes in various model membrane systems.

References

1. G. Szabo, G. Eisenman, R. Laprade, S. M. Ciani and S. Krasne, "Membranes," volume 2, chapter 3, G. Eisenman, ed., Marcel Dekker, Inc., New York (1973).
2. A. Finkelstein and R. Holz, "Membranes," volume 2, chapter 5, G. Eisenman, ed., Marcel Dekker, Inc., New York (1973).
3. D. H. Haynes, A. Kowalsky and B. C. Pressman, J. Biol. Chem., 244, 502 (1969).
4. J. H. Prestegard and S. I. Chan, Biochemistry, 8, 3921 (1969).
5. J. A. Pople, W. G. Schneider and H. J. Bernstein, "High-Resolution Nuclear Magnetic Resonance," McGraw-Hill Book Co., New York (1959).
6. W. Simon and W. E. Morf, "Membranes," volume 2, chapter 4, G. Eisenman, ed., Marcel Dekker, Inc., New York (1973).

PROPOSITION V

It is proposed that Raman spectroscopy can be used to determine the effects of various additives on the structure of the lipid bilayer.

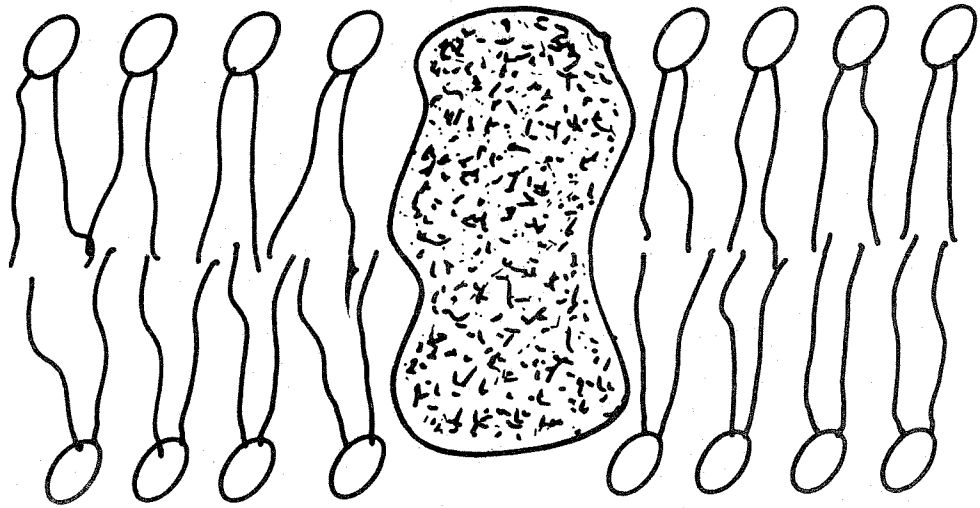
The conformation of the molecules which comprise a lipid bilayer may be significantly affected by the presence of a large additive molecule. A typical amphiphilic lipid molecule can interact with other molecules with exclusively a Van der Waals association, or an electric dipole-dipole or ionic association, or combinations of these interactions. For example, the polar and the ionic regions of proteins may bind to the charged head group of the lipid, whereas the hydrophobic regions of the protein may bind to the lipid hydrocarbon chains. Thus, the additive may cause disorder in the bilayer structure, or it may re-order the lipids into a different conformation, or the additive may have no significant effect on the bilayer structure. These three categories of additive effects are diagrammed in Figure 1.

The functional mechanisms of non-lipid ("additive") components in bilayers may be reflected by the effect of the additive on bilayer structure. Functional mechanisms which require cooperative effects among the bilayer molecules probably occur only if the basic ordering in the bilayer is retained. On this basis, the acetylcholine receptor is not expected to cause extensive disordering of the bilayer. On the other hand, local disorder of the lipid molecules would facilitate diffusion within the bilayer, e. g. rapid reorientation of rhodopsin,

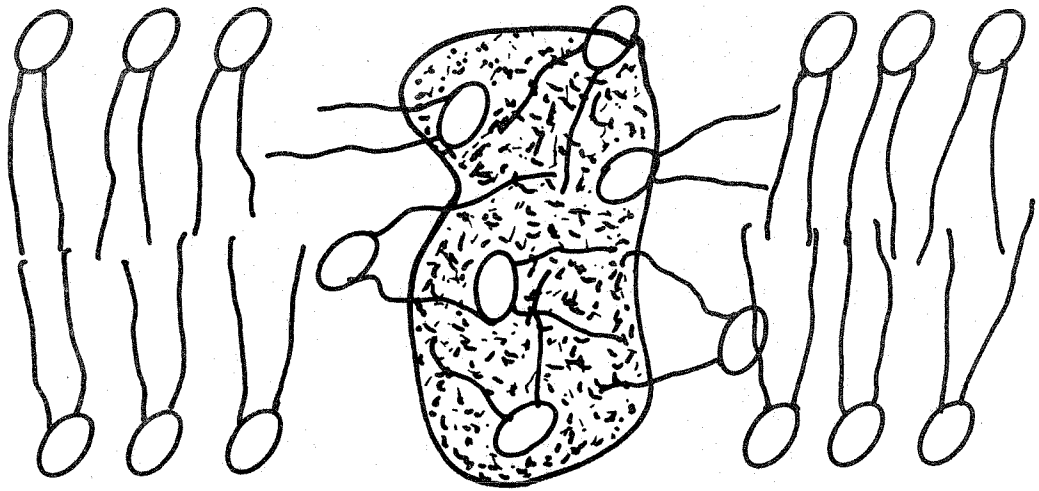
FIGURE 1

Schematic illustration of the effect on the structure of a lipid bilayer of three different varieties of additives.

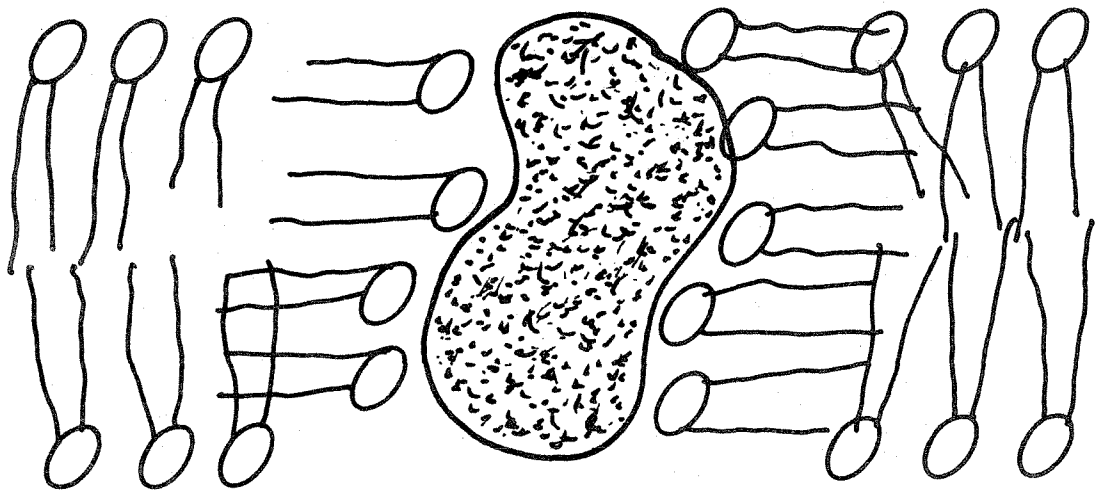
- (A) The additive causes no perturbation of the bilayer structure, and is merely "inserted" into the bilayer.
- (B) The additive causes local disorder among the lipid molecules of the bilayer.
- (C) The additive interacts with the bilayer lipids in such a way as to cause local ordering of the lipid molecules whose hydrocarbon side chains are then parallel to the plane of the bilayer. The unperturbed bilayer lipids have their hydrocarbon chains oriented perpendicular to the plane of the bilayer.



A



B



C

because the additive molecule would not need to break down a stable structure in order to reorient. Finally, an ordered multi-component structure in the bilayer, such as a gramicidin S pore, may be stabilized by local order in the bilayer which is different from the bilayer order farther away from the additive.

The intensity of the lines in a Raman spectrum depends on the alignment of the molecule with respect to the irradiating light and to the direction of detection, unless the polarizability of the molecule is spherically symmetric. (1, 2) This means that the intensity of the lines in the Raman spectrum of a lipid bilayer should be dependent on whether the lipid molecules are parallel, perpendicular, or randomly oriented with respect to the direction of the incident light. Referring to Figure 1, this means that cases (a), (b), and (c) are distinguishable, i. e., the Raman spectrum of bilayer lipids in the presence of an additive will show different line intensities depending on the effects of the additive on the conformation of the lipid molecules.

In addition to the change in intensity of the lines of the Raman spectrum of bilayer lipids, an additive might also cause a slight frequency shift in the lines. Such a frequency shift would be very helpful in quantitatively assessing the additive effects, because then the Raman-active modes corresponding to the lipids near the additive could be distinguished from the bulk of the bilayer lipids.

The Raman spectrum of bilayer lipid molecules which are randomly oriented with respect to the incident light could be obtained

using a standard flat-end capillary cell. The bilayer sample should be of one phase, rather than a dispersion of bilayer particles in water, in order to reduce the amount of (Rayleigh) scattered light.

The spectrum of bilayer lipids which are ordered perpendicular to the incident light can be obtained using the same flat-end capillary cell, by inserting into the bilayer-containing capillary a solid glass rod of diameter just smaller than the capillary inside diameter. Rotating this rod will orient the lipid remaining in the cell so that the hydrocarbon chains are perpendicular to the incident light.

The Raman spectrum of bilayer lipids whose hydrocarbon chains are parallel to the incident light can be obtained by illuminating a stack of thin glass plates between which is sandwiched a thin layer of oriented bilayer. The direction of illumination should be perpendicular to the glass plates.

Experiments on bilayers containing various additives would be performed using the capillary cell with the concentric glass rod. The bulk of the lipid will then be oriented perpendicular to the incident light, and will exhibit the corresponding Raman spectrum. Changes in the intensities of these lines, or the appearance of frequency shifts, would be studied for additives such as the ion-carrier valinomycin, ⁽³⁾ the pore-former gramicidin S, ⁽⁴⁾ the bilayer penetrating cytochrome oxidase, ⁽⁵⁾ the freely reorienting rhodopsin, ⁽⁶⁾ and the bilayer-stiffening cholesterol. ⁽⁷⁾ These Raman spectral effects would be used to develop models for the influence of the

additives on the bilayer structure.

References

1. R. S. Krishnan, "The Raman Effect," volume 1, A. Anderson, ed., Chapter 1, Marcel Dekker, Inc., New York (1971).
2. L. A. Woodward and D. A. Long, Trans. Farad. Soc., 45, 1131 (1949).
3. M.-C. Hsu and S. I. Chan, Biochemistry, 12, 3872 (1973).
4. P. Mueller and D. O. Rudin, Biochem. Biophys. Res. Commun., 26, 102 (1967).
5. P. C. Jost, O. H. Griffith, R. A. Capaldi and G. Vanderkooi, Proc. Nat. Acad. Sci., 70, 480 (1973).
6. P. K. Brown, Nature, New Biol., 236, 35 (1972).
7. D. Chapman, N. F. Owens, M. C. Phillips and D. A. Walker, Biochim. Biophys. Acta, 183, 458 (1969).

